

PROPAGATION OF LONG WAVES IN CURVED DUCTS

A THESIS SUBMITTED TO THE FACULTY OF THE
SCHOOL OF ENGINEERING OF THE
CATHOLIC UNIVERSITY OF LOUVAIN



Get DrA

by

WOJCIECH ROSTAFINSKI

FACILITY FORM 602

N71 - 26338
(ACCESSION NUMBER)

124
(PAGES)

TMX-67184
(NASA CR OR TMX OR AD NUMBER)

(THRU)
G3
(CODE)

07
(CATEGORY)



Reproduced by
**NATIONAL TECHNICAL
INFORMATION SERVICE**
Springfield, Va. 22151

PROPAGATION OF LONG WAVES IN CURVED DUCTS

A Thesis Submitted to the Faculty of the
School of Engineering of the
Catholic University of Louvain
In Partial Fulfillment of the Requirements
for the Degree of
Doctor of Engineering

by

Wojciech Rostafinski

April 1970

Thesis Advisor: Professor F. Buckens

ACKNOWLEDGMENTS

I wish to thank my thesis advisor, Professor F. Buckens, for the suggestion of the problem and for his guidance during the analysis.

I also thank the National Aeronautics and Space Administration, Lewis Research Center, in Cleveland, Ohio, for approval of the overseas training. Particularly, the support and interest of Mr. Hugh M. Henneberry, Chief, Advanced Systems Division, and of Miss Gertrude R. Collins, Training Officer, is gratefully acknowledged.

Above all, I thank my wife Maria for her understanding and encouragement.

TABLE OF CONTENTS

	Page
LIST OF ILLUSTRATIONS.	v
ABSTRACT	vii
INTRODUCTION	1
1.0 GENERAL SOLUTION.	10
1.1 Formulation of the Problem	10
1.10 Equation of motion	10
1.11 Boundary conditions and physical systems to be considered	12
1.2 Determination of the Characteristic Values and of the Characteristic Functions.	15
1.3 Typical Physical Systems.	28
1.30 Infinite bend.	28
1.31 Straight infinite duct	33
1.32 θ_2 radians bend followed by a straight, infinite duct	36
2.0 INTEGRATED SOLUTION	42
2.1 The Characteristic Functions and the Coefficients C	43
2.10 ^m The real root solution	43
2.11 The imaginary roots solutions.	45
2.2 The Infinite Bend	52
2.20 Equations	52
2.21 Discussion	54
2.3 θ_2 Radians Bend Followed by a Straight, Infinite Duct.	62
Motion in the bend	62
3.0 ENERGY FLOW	77
4.0 NUMERICAL APPLICATION	86
4.1 Selection of Parameters	86
4.2 Bessel Functions and Characteristic Functions of the Problem	87
4.21 Solution pertaining to the real root	87
4.22 Solutions pertaining to the imaginary roots of the problems	90
4.3 The Two Physical Systems.	92
4.31 Infinite coil.	93
4.32 90 degree bend followed by a straight duct	96
5.0 CONCLUDING REMARKS AND RECOMMENDATIONS.	102
BIBLIOGRAPHY	105

TABLE OF CONTENTS

	Page
APPENDIX 1	108
APPENDIX 2	109
APPENDIX 3	111
APPENDIX 4	113

LIST OF ILLUSTRATIONS

	Page
1. The Two Physical Systems Considered	14
2. $\cos\left[\mu_m \ln \frac{r}{R_1}\right]$ for $m = 1, 2, 3$ and 4	55
3. Tangential Vibrational Velocities of the Propagating Long Waves in Curved Ducts	57
4. Propagation of Long Waves in Curved Ducts	57
Curve A: Relation Between the Sharpness of the Bend and the Radial Location of the Average Tangential Velocity v_0	
Curve B: Comparison of the Phase Velocity in Bends with the Phase Velocity in Straight Ducts.	
5. Attenuated Tangential Vibrational Velocities at Bend's Inlet at Three Different Angular Positions	57
6. Attenuated Tangential Vibrational Velocities for Three Different Bends	60
7. Standing Radial Vibrational Velocities in Bends	60
8. Attenuated Radial Vibrational Velocities at Bend's Inlet	60
9. Transmission of Acoustic Waves through Elbows, Experimental data by Lippert.	84
10. Bessel Functions of Fractional and Imaginary Order.	89
11. Infinite Coil, Distribution of Vibrational Velocities	94
12. 90° Bend Followed by a Straight Duct, Distribution of Vibrational Velocities	98
13. Propagation in Bend-Straight Duct System. Changes in Location of the Average Tangential Vibrational Velocity v_0	100
14. Propagation in Bend-Straight Duct System. Tangential Vibrational Velocities at the Bend's Curved Walls, at $r = R_1$ and $r = R_2$	100

15. The Matrix of Integrals

$$\Lambda_{mn} = \int_{R_1}^{R_2} \cos \left[\zeta_n (r - R_1) \right] \cos \left[\mu_m \ln \frac{r}{R_1} \right] dr \dots \quad 117$$

ABSTRACT

Propagation of long waves in a two dimensional systems is analysed. An acoustic approximation is used and boundary conditions simulating typical industrial piping systems are formulated. The thesis consists of three main parts. In the first part a general solution of the boundary value problem is obtained. In the second part series solutions of the equations of motion are generated, and a physical interpretation of results is given. A numerical application and a discussion of the problem are given in the last part.

INTRODUCTION

The characteristics of motion of a fluid, whether steady or unsteady, depend on the nature of the fluid, the imposed initial conditions and on the nature of the system in which the motion takes place. In the large class of unsteady motions of compressible fluids, the periodic motion or wave propagation is particularly important from the point of view of both pure and applied sciences and has been the subject of extensive analysis. However, except for essentially simple systems the motion of pressure waves is very complex. Generally, the waves may be reflected, diffracted and distorted. They may be subject to attenuation and decay or to inhomogeneous distribution. The more the symmetry of a system departs from a simple rectangular, cylindrical or spherical geometry and the more the initial conditions differ from that appropriate to the boundary, the more these effects will be pronounced.

Besides a purely scientific interest in the problem of propagation of waves, there are many engineering reasons for a better understanding of wave motion. Of theoretical and practical interest is the determination of the basic modes of motion and their phase and group velocities. Also knowledge of the resonant and the cut-off frequencies as well as the determination of the reflection and transmission coefficients are of substantial interest.

Propagation of waves in curved ducts and pipes belong to the class of motion which is characterized by wave patterns totally different from those known in straight ducts or in unlimited space.

The curvilinear boundaries are responsible for the appearance of a continuous standing radial wave which in turn affects the transmitted tangential waves. The propagation in curvilinear waveguides or bent ducts is difficult to analyze, and mathematical models developed to date are complicated. Perhaps that is one of the reasons why relatively few papers are available on this subject.

The purpose of this treatise is to solve the problem of propagation of waves in curved ducts. It is intended to obtain a solution for long acoustic waves in slightly and sharply bend ducts. This problem has been only partially analyzed by various authors.

The first recognition of the problem of propagation of pressure waves in a curved conduit, as distinct from the motion in a straight line, was formulated by Rayleigh⁽¹⁾. In a short, brilliant expose he demonstrated that long waves in a curved pipe of infinitesimal cross section behave exactly as in a straight pipe. The curvature of the pipe is of no importance. His analysis is based on the linearized equation of motion and conclusions are not valid if the cross section of the pipe is finite. However, what is important is that he establishes a limit to which equations describing wave motion in pipes of arbitrary shape must tend.

Subsequent research of wave motion in curvilinear ducts is almost exclusively analytical!. The majority of papers treat the propagation of electromagnetic waves in curved ducts. Only a few discuss the propagation of sound waves. Interestingly enough, along with analytical formulation of the behavior of waves in bends there

appeared a series of papers dealing with mathematics needed to solve the physical problem of waveguides. This parallel effort indicates that the solution of the problem of bent waveguides requires mathematical formulations and techniques not generally available.

To review the literature on the wave propagation in curved ducts it is desirable to discuss the work done by grouping studies by adopted boundary conditions. In several instances studies originally intended to be general were actually reduced to some specific, restricted cases by simplification of boundary conditions in order to solve the problem.

In 1905 Kalahne⁽²⁾ and in 1946 Jouguet⁽³⁾ and a decade later Karpman⁽⁴⁾ considered oscillations in rigid toroids. Jouguet approaches the problem by the method of perturbations while Kalahne and Karpman use the method of separation of variables. Both Jouguet and Karpman intended to study propagation but simplified the problem by adopting closed systems. A similar standing wave problem, using a configuration of an elbow connected to two segments of straight tube, was treated in 1930 by Matchinski⁽⁶⁾. A very extensive and complete treatment of the behavior of electromagnetic standing waves in circular cross sections of simple or coaxial tubes is given in the text "Electromagnetic Waveguides and Cavities" by Goubau⁽⁵⁾.

As interesting as their developments are they contribute little to the determination of parameters of progressing waves. However, a number of papers published between 1939 and 1969 did contribute to the problem. Buchholz⁽⁷⁾, using separation of variables

obtains a solution for propagation of electromagnetic waves in slightly bent waveguides of infinite length. He calculates an expression for a wave propagation constant and draws several general conclusions about behavior of waves in bends. Buchholz's paper is the first contribution to the problem of progressive waves. The problem of the infinitely long bend was also treated by Krasnushkin⁽⁸⁾, Grigor'yan⁽⁹⁾, and by Victorov and Zubova⁽¹⁰⁾. Krasnushkin approaches the problem by the method of separation of variables but in view of mathematical difficulties proposes a perturbation method and treats the simplified case of the slightly bent tubes. Grigor'yan solves the differential equation by expansion of the cross-product of Bessel functions into a Taylor series. He tries to obtain an algorithm of sufficient generality to be applicable to all possible impedances of the waveguide walls. Coefficients of his series consists of a sequence of Wronskians as determined by Basset⁽¹¹⁾. The method is only partially successful. Grigor'yan obtains correct general information on amplitude and distribution of the radial oscillations but his basic mode wave number does not verify the differential equation except for the Raleigh case of very narrow pipe.

Victorov and Zubova treat short wave propagation in a solid layer and outline a possible solution for an infinite coil of large radius of curvature. Finally, Voskresenskin⁽¹²⁾ and Sveshnikov et al.⁽¹³⁾ approach the problem of infinite bend using the separation of variables. However, like several other authors, they do not solve their equations but limit themselves to general discussion.

The contributions to the solution of wave propagation in curved ducts which were reviewed considered only one aspect of the problem, the functions which depend on radii and on boundary conditions of the bend walls. The dependence on the longitudinal coordinate, that is, the angular propagation was greatly simplified by assuming an endless coil. However, two papers consider the angular dependence in detail. Rice⁽¹⁴⁾, using matrix equations establishes the basic mode propagation constant for electromagnetic waves and calculates the coefficient of reflection of waves incident upon a bend. Basically, he treats a junction between a straight and a curved cylindrical duct. His procedure - the theory of matrices - is an obvious choice for a system capable of supporting several modes of wave motion. Arlinger⁽¹⁵⁾, using the method of perturbation, presents a problem of compressible potential flow in a bend of a duct of circular cross section. Although this is not a case of propagation of waves, Arlinger's general solution for potential motion in a bend and at a junction is closely related to our problem. The common feature of the two papers is need for extensive supporting mathematics. Both authors obtain solutions which contain definite integrals which cannot be integrated by ordinary means. To by-pass this technical difficulty Rice supplies tabulated values in an appendix. Arlinger resorts to integration by Simpson's rule.

A number of papers on roots of equations containing cylindrical functions, (cross-products of Bessel functions) were found in the process of verifying the existing literature on the wave motion in

cylindrical coordinates. Unfortunately most of these papers, (by McMahon⁽¹⁶⁾, Truell⁽¹⁷⁾, Dwight⁽¹⁸⁾ and Kline⁽¹⁹⁾) are limited to research of characteristic values of the argument of the Bessel functions. Therefore, their usefulness is limited to problems concerned with finding resonant conditions in closed systems. However, one monograph by Buckens⁽²⁰⁾, does apply directly to relationships for evaluating the order of cross products of Bessel functions of real and of imaginary order, and was used in developing the expressions for decaying oscillations.

Among the few treatises on propagation of sound in bends are those by Miles^(21,22) in which he establishes an analogy between propagation of sound and an electrical transmission line are most important. The method is then applied to a right angle joint of rectangular tubes. Actually, Miles is considering a mitered 90° bend with the outside corner chamfered. This greatly simplifies his analysis. Bends of this type are discussed by Goubau⁽⁵⁾ and of course constitute a special case of "reflectionless" bends which may be used for a selective range of frequencies.

The work of Miles was successfully checked by Lippert⁽²³⁻²⁵⁾. Lippert presents an experimental study of sound wave propagation in mitered bends of various angles. The experiments were conducted over a wide range of frequencies and show that long waves in mitered bends propagate with insignificant reflections. In an interesting experiment with a rounded 90° bend (the outside wall of the miter joint of the duct was made circular with a radius equal to the duct

width) Lippert shows that the transmissivity was far superior to that of an ordinary miter joint over a very wide range of frequencies. Finally, it should be mentioned that Morse and Feshbach⁽²⁶⁾ propose an approximate method for the solution of the problem of long wave propagation in a two-dimensional 90° miter bend. A series solution of the wave equation is written for the two infinite branches of the two-dimensional duct. The square area of the elbow proper is analyzed by the method of conformal transformation.

An analytical and experimental program on wave propagation in flexible pipes was carried out by NASA⁽²⁷⁾. Propagation of small sinusoidal perturbations was studied in a line including a 90° elbow with flexible supports. The experiments were supported by an analysis based on the acoustic impedance theory which described the dynamic behavior of the system. The conclusion of the experiments is that the elbow created no noticeable effects.

Propagation of waves in bends and more particularly in circular bends still requires fundamental analysis. The, thus far, obtained algorithms for computation of the wave motion are very cumbersome and the past research covers only certain aspects of the wave motion in curved bends.

The general object of this dissertation is to analyze the behavior of long waves in curved conduits. The purpose of the analysis is to determine the distribution and variation of the vibrational velocities, and the phase of motion, at any point in the systems under consideration. The particular problem is to determine a

mathematical model of the wave motion that will yield, with reasonable accuracy, meaningful answers and allow a physical interpretation of results

To satisfy these requirements the propagation of acoustic waves was selected for model. The wave transmission through bends of arbitrary sharpness is solved, for the first time, as boundary value problem using the characteristic functions.

The following conditions are assumed to exist. There is a sustained, continuous and steady propagation of long acoustic waves in a two-dimensional curved channel. Long acoustic waves are understood to be harmonic vibrations of infinitely small amplitude of a compressible, inviscid fluid. The wavelength is at least two orders of magnitude larger than the width of the channel. The pressure distribution within the channel satisfies the wave equation. The radius of curvature of the bends is unrestricted.

In this study two acoustic systems are considered which allow determination of the basic modes of motion and describe the transition and distortion of plane waves as they propagate down the curved channel. A detailed study of the behavior of waves in junctions between straight and curved ducts will be given.

The mathematical treatment of the problem utilizes the method of separation of variables. Solutions and expressions for principal modes of the wave are obtained by using the linearized equation of motion solved for its characteristic values.

This original approach required a novel use of Bessel functions

to determine the characteristic values of the steady and the decay-
ing fields of motion.

The unavoidable approximations in the numerical solutions of
the cylindrical functions are due to use of series expansion of Bes-
sel functions and from restrictions necessary to solve infinite ma-
trices.

1.0 GENERAL SOLUTION

1.1 Formulation of the Problem

1.10 Equation of motion. - Because the complexity of the problem considered requires a simplified mathematical model, a linear equation of motion, the wave equation,

$$\nabla^2 \phi = \frac{1}{c^2} \frac{\partial^2 \phi}{\partial t^2} \quad (1.1)$$

will be used. It is generally tractable and should yield results approximating, to a degree, the real phenomena in curved pipes. Equation (1.1) is well known and there is no necessity to derive it. It is, however, important to indicate here the usually omitted discussion of the degree of approximation resulting from use of a linearized equation and the nature of applied assumptions. The best way to present all approximations and assumptions is to derive the wave equation from a most general equation of motion.

The derivation given hereafter is classical. Elements of it may be found in most of the advanced texts⁽²⁸⁾⁽²⁹⁾. The most complete derivation is given by Morse and Feshbach⁽²⁶⁾.

The sum of forces on a fluid element equals the acceleration of the element, $D\bar{V}/Dt$, times its mass $\rho \, dx \, dy \, dz$.

The very general equations of motion, without restrictions, as to the compressibility, viscous forces, and turbulence, is

$$\rho \frac{D\bar{V}}{Dt} = -\nabla(P + W) + \nabla \cdot \bar{\tau} \quad (1.2)$$

$\frac{D\bar{V}}{Dt}$ is the substantial derivative of velocity vector, a sum of the

local contribution to acceleration $\frac{\partial \bar{V}}{\partial t}$ and the convective contribution due to translation

$$\frac{d\bar{V}}{dt} = \bar{V} \cdot \nabla \bar{V} = \frac{1}{2} \nabla (\bar{V} \cdot \bar{V}) - \bar{V} \times \text{curl } \bar{V} = \frac{1}{2} \nabla V^2 - \bar{V} \times \text{curl } \bar{V}$$

The $-\nabla W = \bar{F}$ is the external potential of conservative forces of gravity and $\nabla \cdot \bar{\tau}$ is the viscous force on element per unit volume but because of the tensorial nature of $\bar{\tau}$, $\nabla \cdot \bar{\tau}$ is not a simple divergence.

To simplify the problem we restrict our analysis to small amplitude displacements and velocities. We also assume that the compressible fluid under consideration exhibits no free surface, is homogeneous throughout the domain. In this case all terms in equation (1.2) involving V^2 can be neglected and, assuming that the compressional viscosity will be small, the influence of viscosity will be negligible. Furthermore, in the equation of motion of a homogeneous fluid, in the absence of a free surface, the forces due to the external potential (gravity) can be disregarded if pressure P is the excess pressure p over that of the fluid at rest, P_0 . With these assumptions, the equation of motion reduces to

$$\rho \frac{\partial \bar{V}}{\partial t} = - \nabla p \tag{1.3}$$

Now we may write $\bar{V} = \text{grad } \phi$ where $\phi(x,y,z,t)$ is a scalar function or potential whose partial derivatives with respect to x,y,z are the components of velocity \bar{V} in those directions. Substituting, differentiating equation (1.3) with respect to time and since

$$\frac{\partial p}{\partial t} = -\frac{1}{\chi} \operatorname{div} \bar{v} \quad \text{as established in appendix 1, equation (A1.1),}$$

the equation of motion for small oscillations of a compressible, homogeneous and inviscid fluid at rest is

$$\nabla^2 \phi = \frac{1}{c^2} \frac{\partial^2 \phi}{\partial t^2} \quad (1.1)$$

where $c^2 = 1/\chi\rho$. This is the linearized wave equation in terms of the velocity potential. It will be convenient to express equation (1.1) in polar coordinates to fit the geometry of circular curved pipes.

The two-dimensional equation of motion of the analytical model is then

$$\frac{\partial^2 \phi}{\partial r^2} + \frac{1}{r} \frac{\partial \phi}{\partial r} + \frac{1}{r^2} \frac{\partial^2 \phi}{\partial \theta^2} = \frac{1}{c^2} \frac{\partial^2 \phi}{\partial t^2} \quad (1.4)$$

The particle velocities (the vibrational velocities) are given by

$$v(r, \theta, t) = \frac{1}{r} \frac{\partial \phi}{\partial \theta} \quad (\text{the tangential component})$$

$$u(r, \theta, t) = \frac{\partial \phi}{\partial r} \quad (\text{the radial component})$$

and the excess pressure by

$$p(r, \theta, t) = -\rho \frac{\partial \phi}{\partial t} .$$

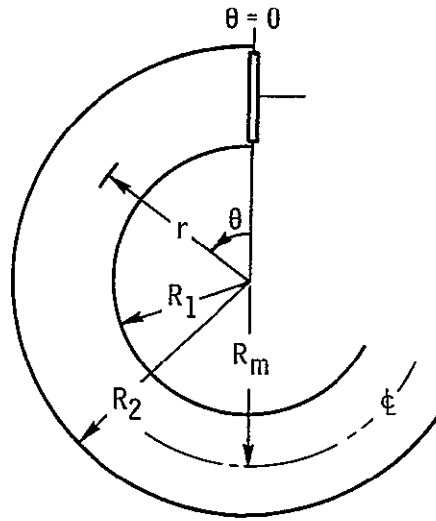
1.11 Boundary conditions and physical systems to be considered. - The

boundary conditions which the solution must satisfy depend on the physical configuration of the system to be analyzed. On the other hand we are not entirely free to choose any boundary conditions

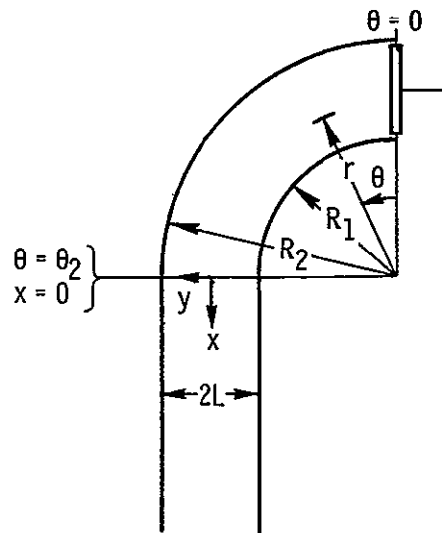
because the solution of the hyperbolic equation to have a physical meaning must be done over an open boundary at least in one space dimension which may be along the time axis. In the case of the propagation of waves in pipes the walls are a closed boundary, the origin and the far end sections may be opened or closed. The time axis is usually open. On the walls and on the end sections the Dirichlet and the Neumann conditions may be used. The Dirichlet condition requires that the potential be specified on the boundary. The Neumann condition requires that the normal component of the velocity, on the boundary be specified.

Two physical systems shown on figure 1 will be considered. Both approximate typical industrial piping. The first consists of a rigid infinite bend approximating a coil. At the inlet section of the coil pulsations are generated by a hypothetical piston of infinitesimal displacements. Conditions at the far end section of the bend are of no consequence because assumption of an infinite coil implicitly states that the far end section condition will not contribute to the solution; only a simple wave in a positive θ direction will be considered.

The second system consists of a circular bend followed by a straight, infinite duct. As in the case of the infinite coil, at the inlet section of the bend pulsations are generated by a hypothetical piston of infinitesimal displacement. The far end of the system will be at infinity. The system of coordinates and nomenclature used are shown on figure 1.



(a) Infinite bend.



(b) 90° Bend followed by an infinite straight duct.

Figure 1 - The two physical systems considered.

It will be assumed that the walls of the curved and the straight ducts will be perfectly rigid so that the Newman condition will apply. Generally, walls may have an admittance (reciprocal of the normal impedance) different from zero and a very general solution may be obtained on such a basis. An extensive discussion of this aspect of the boundary conditions and formulation of this problem may be found in Grigor'yan's paper⁽⁹⁾. Our assumption of perfectly stiff walls and hence, the requirement that, at the walls, the normal component of the vibrational velocity vanishes is a very good approximation of actual acoustic systems.

1.2. Determination of the Characteristic Values and of the
Characteristic Functions

The linearized wave equation in cylindrical coordinates is known to be separable in coordinates proper for the boundary. Equation (1.4) may be broken up into a set of ordinary differential equations, each including a separation constant. Consequently, no other method of solving our boundary value problem will be contemplated in spite of the fact that several approximate methods, such as the method of perturbation, have been found useful and leading to meaningful, although generally, restricted results.

To solve equation (1.4), we assume a solution of the form

$$\phi = R(r)\theta(\theta)T(t)$$

By separation of variables we have

$$\frac{1}{c^2} \frac{T''}{T} = -k^2 \quad \text{and} \quad T = e^{i(kct+\alpha)} = e^{i(\omega t+\alpha)}$$

This solution assumes that the dependence on time is simple harmonic (with a possible phase lag α) and that equation (1.4) is, in fact, a scalar Helmholtz equation.

Next, $\frac{\theta''}{\theta} = -v^2$ The solution of the angle depending term may be periodic or linear, depending on the value of the separation constant.

$$\theta = a_v \cos v\theta + b_v \sin v\theta \quad v \neq 0$$

$$\theta = c\theta + d \quad v = 0$$

$$\text{Finally, } R'' + \frac{1}{r^2} R' + k^2 - \frac{v^2}{r^2} R = 0$$

and

$$R = A_v J_v(kr) + B_v Y_v(kr)$$

which is the characteristic function of the problem.

Superposition of solutions is allowed; for equation (1.4) is linear and a general solution may be written in the form

$$\begin{aligned} \phi = \int_C e^{i(\omega t + \alpha)} (a_v \cos v\theta + b_v \sin v\theta) [A_v J_v(kr) + B_v Y_v(kr)] dv \\ + e^{i(\omega t + \alpha)} (c\theta + d) [A_0 J_0(kr) + B_0 Y_0(kr)] \end{aligned} \quad (1.5)$$

where C is a set of points in the complex plane, to be determined in order to satisfy the boundary conditions.

The solution for $v = 0$ might have been included in the integral terms but in order to show more explicitly the linear dependence on θ of this solution, it has been written separately.

Before proceeding with application of the boundary conditions we will consider the well known technique of splitting the potential field into the incident and the scattered waves

$$\phi = \phi_i + \phi_s$$

The incident plane waves $\phi_i = v_0 \exp i(\omega t - kr \sin \theta)$ propagate from the vibrating pistons into the bend until they strike the curved wall facing the piston. However, shortly after leaving the piston, the waves cease to be plane because they will be strongly diffracted on the curved inner wall of the bend. It is noted here that the work on diffraction of long waves by the edge of a semi-finite screen by Lamb⁽²⁸⁾ in 1906, and generalized by Penny and Price in 1952⁽³⁰⁾, is not valid on curved walls.

The reflected, scattered waves which will result from the impact on the outer curved wall, will form cusped fronts which have been experimentally studied by Wood⁽³¹⁾. These fronts will carry the energy of original waves down the bend. As the front progresses down the bend it will spread, and assume some new form. The initial condition of the reflected wave is that of the diffracted wave reaching the outer curved wall. Because the degree of diffraction of the plane waves is unknown, the initial conditions of the reflected wave are undeterminable. In view of the difficulty of obtaining proper expressions for the incident and the reflected waves, this approach is not applicable. Consequently, the case of motion in bent ducts (which lack axial symmetry leading to the diffraction

of waves and multiple, endless reflections) requires a solution which would not include the identification of the component waves.

To satisfy the partial differential equation and the boundary conditions for perfectly rigid circular walls, a characteristic equation will be found whose roots will be the characteristic values of the problem: a set of values of the separation parameter ν which will yield a nontrivial solution of the problem. Differentiating equation (1.5) with respect to r and equating to zero we obtain for the two circular boundaries

$$A_{\nu} J'_{\nu}(kR_1) + B_{\nu} Y'_{\nu}(kR_1) = 0 \quad \nu \neq 0 \quad (1.6a)$$

$$A_{\nu} J'_{\nu}(kR_2) + B_{\nu} Y'_{\nu}(kR_2) = 0$$

$$A_0 J'_0(kR_1) + B_0 Y'_0(kR_1) = 0 \quad \nu = 0 \quad (1.6b)$$

$$A_0 J'_0(kR_2) + B_0 Y'_0(kR_2) = 0$$

Conditions equation (1.6b) give $B_0 = -A_0 \frac{J'_0(kR_1)}{Y'_0(kR_1)}$

$$\text{and } J'_0(kR_1)Y'_0(kR_2) - J'_0(kR_2)Y'_0(kR_1) = 0 \quad (1.7a)$$

Since $J'_0(kr) = J_1(kr)$ and $Y'_0(kr) = -Y_1(kr)$, equation (1.7a) can be written

$$J_1(kR_1)Y_1(kR_2) - J_1(kR_2)Y_1(kR_1) = 0 \quad (1.7b)$$

For the case of (kr) greater than the first root of $Y_1(kR_1)$ the cross-product (eq. (1.7b)) will yield a series of solutions. In the present case where $0 < (kr) < (kR_2) \ll 1$, with the steep slope of

$Y_1(kr)$ and relatively moderate increase of $J_1(kr)$ over the range (kR_1) to (kR_2) , there is no solution for equation (1.7b) in the range under consideration.

Consequently, the solution $v = 0$ cannot be considered. Equations (1.6a) give

$$B_v = -A_v \frac{J'_v(kR_1)}{Y'_v(kR_1)}$$

$$\text{and } J'_v(kR_1)Y'_v(kR_2) - J'_v(kR_2)Y'_v(kR_1) = 0 \quad (1.8)$$

Considering $R_2 = aR_1$ ("a" is a proportionality constant) and using the relation

$$Y'_v(kr) = \frac{\cos(\pi v) J'_v(kr) - J'_{-v}(kr)}{\sin(\pi v)}$$

equation (1.8) simplifies to

$$\frac{1}{\sin \pi v} \left[J'_v(kR_1)J'_{-v}(aR_1) - J'_v(aR_1)J'_{-v}(kR_1) \right] = 0 \quad (1.9)$$

There are no known tables for the roots v_m of the characteristic equation (1.9). To evaluate the v_m 's we expand the J'_v and J'_{-v} in terms of increasing powers of the argument (aR_1) and (kR_1) . If we limit the expansion in the first approximation to the first term:

$$J'_v(kr) \approx \frac{v}{2^v \Gamma(v+1)} (kr)^{v-1} + \dots$$

$$J'_{-v}(kr) \approx \frac{v}{2^{-v} (1-v)} (kr)^{-v-1} + \dots$$

and substitute into equation (2.5) we obtain

$$\frac{v^2}{\sin \pi v \Gamma(v+1) (1-v)} \left[(kR_1)^{-v-1} (kaR_1)^{v-1} - (kR_1)^{v-1} (kaR_1)^{-v-1} \right] = 0$$

and finally

$$\frac{v}{\pi(kR_1)^2} \left(a^{v-1} - a^{-v-1} \right) = 0 \quad (1.10)$$

Solution $v = 0$ has been already rejected. Therefore, the only acceptable solution must satisfy the equation

$$a^{v-1} = a^{-v-1}$$

which may be put in the form

$$a^{2v} = 1 \quad \text{or} \quad e^{2v \ln a} = 1$$

Hence, $2v \ln a = 2m\pi i$

$$\text{that is } v_m = \frac{m\pi i}{\ln a} \quad (m = 1, 2, 3 \dots) \quad (1.11)$$

Better approximations will be given by the second and following terms of expansion of J'_v and J'_{-v}

$$J'_v(z) = \frac{v(z)^{v-1}}{2^v \Gamma(v+1)} - \frac{(2+v)z^{1+v}}{2^{2+v} (2+v)} + \frac{(4+v)z^{3+v}}{2^{4+v} \Gamma(3+v) \Gamma(3)} - \dots \quad (1.12)$$

$$J'_{-v}(z) = \frac{-v z^{-v-1}}{\Gamma(1-v) 2^{-v}} - \frac{(2-v)z^{1-v}}{2^{2-v} \Gamma(2-v)} + \frac{(4-v)z^{3-v}}{2^{4-v} \Gamma(3) \Gamma(3-v)} - \dots$$

Since $z = kr$ is small for k small, we neglect here the third term of these expansions.

Equation (1.9) gives:

$$\left[\frac{(kR_1)^{\nu-1}}{2^\nu \Gamma(\nu+1)} - \frac{(2+\nu)(kR_1)^{1+\nu}}{2^\nu \cdot 4\Gamma(2+\nu)} \right] \left[\frac{-\nu(kR_1)^{-\nu-1}}{(1-\nu)2^{-\nu}} - \frac{(2-\nu)(kR_1)^{1-\nu}}{2^{-\nu} \cdot 4 \cdot \Gamma(2-\nu)} \right]$$

$$- \left[\frac{(kR_1)^{\nu-1}}{2^\nu \Gamma(\nu+1)} - \frac{(2+\nu)(kR_1)^{1+\nu}}{2^\nu \cdot 4\Gamma(2+\nu)} \right] \left[\frac{-\nu(kR_1)^{-\nu-1}}{\Gamma(1-\nu)2^{-\nu}} \right.$$

$$\left. - \frac{(2-\nu)(kR_1)^{1-\nu}}{4 \cdot 2^{-\nu} \Gamma(2-\nu)} \right] = 0 \quad (1.13)$$

where,

$$\Gamma(\nu+1) = \nu\Gamma(\nu)$$

$$\Gamma(1-\nu) = \frac{\pi}{\sin \pi\nu} \frac{1}{\Gamma(\nu)}$$

$$\Gamma(2+\nu) = (1+\nu)\Gamma(1+\nu) = \nu(1+\nu)\Gamma(\nu)$$

$$\Gamma(2-\nu) = (1-\nu)\Gamma(1-\nu) = (1-\nu)\pi/\sin(\pi\nu) \cdot \Gamma(\nu)$$

$$\Gamma(1-\nu) = -\nu\Gamma(-\nu)$$

$$\Gamma(1+m+\nu) = (1+\nu)(2+\nu) \dots (m+\nu)\Gamma(1+\nu)$$

After algebraic manipulations and dropping the term containing the $(kR_1)^2$ we have

$$\frac{\sin \pi\nu}{16\pi\nu(1+\nu)(1-\nu)} \left\{ + \nu(1-\nu)(2+\nu) \left(a^{-\nu-1} - a^{1+\nu} \right) + (1+\nu)(2-\nu) \right.$$

$$\left. \nu \left(a^{\nu-1} - a^{1-\nu} \right) + 4\nu^2(1-\nu)(1+\nu)(kR_1)^{-2} \left(a^{\nu-1} - a^{-\nu-1} \right) \right\} = 0 \quad (1.14)$$

In order to improve on the first approximation, (eq. (1.11)),

we now assume

$$v = \frac{m\pi i}{\ln a} + \frac{\ln(1 + \epsilon_m)}{\ln a} \quad (1.15)$$

where ϵ_m is a small quantity.

Solving and remembering that

$$\ln z = \ln|z| + i(\arg z + 2n\pi) \quad n = 0, \pm 1, \dots$$

we have

$$\begin{aligned} 0 &= (1 - v)(2 + v) \left(e^{-m\pi i - \ln a} - e^{m\pi i + \ln a} \right) \\ &+ (1 + v)(2 - v) \left(e^{m\pi i - \ln a} - e^{-m\pi i + \ln a} \right) \\ &+ 4v(1 - v)(1 + v)(kR_1)^{-2} \left(e^{m\pi i + \ln(1+\epsilon)\ln a} - e^{-m\pi i - \ln(1+\epsilon) - \ln a} \right) \\ 0 &= (1 - v)(2 + v)(-1)^m \left(a^{-1} + a^{+1} \right) + (1 + v)(2 - v)(-1)^m \left(a^{-1} - a^{+1} \right) \\ &+ 4v(1 - v)(kR_1)^{-2} (-1)^m \frac{1 + \epsilon}{a} - \frac{1}{a(1 + \epsilon)} \end{aligned}$$

since $\frac{1}{1 + \epsilon} \cong 1 - \epsilon$

$$(2 - v^2) \left(a^{-1} - a^{+1} \right) + 2v(1 - v^2)(kR_1)^{-2} \frac{2\epsilon}{a} = 0$$

$$\epsilon_m = - \frac{(2 - v^2)(kR_1)^2}{4v(1 - v^2)} (1 + a^2)$$

$$\epsilon_m = -i \frac{(kR_1)^2 (a^2 - 1) \left[2 + \frac{m^2 \pi^2}{(\ln a)^2} \right]}{4m\pi \left[1 + \frac{m^2 \pi^2}{(\ln a)^2} \right]} \ln a \quad (1.16)$$

and

$$v_m = i \left\{ \frac{\frac{m\pi}{\ln a} - \frac{(kR_1)^2(a^2 - 1) \left[2 + \frac{m^2\pi^2}{(\ln a)^2} \right]}{4m\pi \left[1 + \frac{m^2\pi^2}{(\ln a)^2} \right]}} \right\} \quad (1.17)$$

$$m = 1, 2, 3$$

$$\text{For } m = 0 \quad v_0 = \frac{\ln(1 + \epsilon_0)}{\ln a}$$

Substituting into equation (1.14) and neglecting terms in v_0^2 we

have

$$\begin{aligned} & \left[\left(2 - \frac{\ln(1 + \epsilon_0)}{\ln a} \right) \frac{1}{a(1 + \epsilon_0)} - a(1 + \epsilon_0) \right. \\ & + \left. \left[2 + \frac{\ln(1 + \epsilon_0)}{\ln a} \right] \left(\frac{1 + \epsilon_0}{a} - \frac{a}{1 + \epsilon_0} \right) \right. \\ & \left. + 4 \frac{\ln(1 + \epsilon_0)}{\ln a} (kR_1)^{-2} \left(\frac{1 + \epsilon_0}{a} - \frac{a}{a(1 + \epsilon_0)} \right) \right] = 0 \end{aligned} \quad (1.18)$$

Solving, we have

$$\begin{aligned} & \left(2 - \frac{\ln(1 + \epsilon_0)}{\ln a} \right) \frac{1 - \epsilon_0}{a} - a(1 + \epsilon_0) + \left(2 + \frac{\ln(1 + \epsilon_0)}{\ln a} \right) \frac{1 + \epsilon_0}{a} \\ & - a(1 - \epsilon_0) + 4 \frac{\ln(1 + \epsilon_0)}{\ln a} (kR_1)^{-2} \frac{2\epsilon_0}{a} = 0 \\ & -4 \left(a - \frac{1}{a} \right) + 2 \frac{\ln(1 + \epsilon_0)}{\ln a} \epsilon_0 \left(a + \frac{1}{2} \right) + \frac{8\epsilon_0}{a} \frac{\ln(1 + \epsilon_0)}{\ln a} (kR_1)^{-2} = 0 \end{aligned}$$

Finally

$$\frac{\epsilon_0 \ln(1 + \epsilon_0)}{\ln a} = \frac{2 \left(a - \frac{1}{2} \right)}{-\frac{4}{a} (kR_1)^{-2} + a + \frac{1}{a}}$$

$$\ln(1 + \varepsilon) \cong \varepsilon$$

$$\frac{\varepsilon_0^2}{\ln a} = \frac{2(a^2 - 1)}{4(kR_1)^{-2} + a^2 + 1}$$

and

$$v_0 = \sqrt{\frac{2(a^2 - 1)/\ln a}{4(kR_1)^{-2} + a^2 + 1}} \quad (1.19)$$

Since the result depends on v_0^2 we retrace our steps and solve equation (1.18) without neglecting terms in v_0^2 . After algebraic manipulations we obtain a new expression for v_0

$$v_0 = \sqrt{\frac{2(a^2 - 1)/\ln a}{4(kR_1)^{-2} + a^2 + 1 + \frac{a^2 - 1}{\ln a}}} \quad (1.20)$$

There is an infinite set of pure imaginary roots v_m given by equation (1.17) and one single real root given by equation (1.20). The uniqueness of the obtained real root remains to be verified. Expanding equation (1.9) by means of series (1.12) and substituting for a^v the power series $a^v = 1 + v \ln a + \frac{v^2(\ln a)^2}{2} \dots$ we obtain, in the first approximation,

$$v_0 = \sqrt{\frac{2 \frac{a^2 - 1}{\ln a}}{4(kR_1)^{-2}}} = (kR_1) \sqrt{\frac{a^2 - 1}{2 \ln a}}$$

This result was obtained with only first two terms of the series for a^v . When three terms of this series are used and when small

of the fourth order are neglected, we obtain

$$v_0 = \sqrt{\frac{2 \frac{a^2 - 1}{\ln a}}{4(kR_1)^{-2} + a^2 + 1 + \frac{a^2 - 1}{\ln a} - (a^2 - 1) \ln a}}$$

Equation (1.20) is thus verified by series expansion and uniqueness of the root v_0 established. Adding all solutions obtained with each of the calculated root, equation (1.5) becomes

$$\phi = \sum_{m=0}^{\infty} e^{i\omega t} \left(a_{v_m} \cos v_m \theta + \sin v_m \theta \right) \left[A_{v_m} J_{v_m}(kr) + B_{v_m} Y_{v_m}(kr) \right] \quad (1.21)$$

and using the previously determined value of B_{v_m} in terms of A_{v_m}

$$B_{v_m} = -A_{v_m} \frac{J'_{v_m}(kR_1)}{Y'_{v_m}(kR_1)}, \text{ and simplifying notation by adopting}$$

$$C_{v_m} = -\frac{A_{v_m}}{Y'_{v_m}(kR_1)}$$

we obtain

$$\phi = e^{i\omega t} \sum_{m=0}^{\infty} C_{v_m} \left(a_{v_m} \cos v_m \theta + \sin v_m \theta \right) \left[-Y'_{v_m}(kR_1) J_{v_m}(kr) - J'_{v_m}(kR_1) Y_{v_m}(kr) \right]$$

which still further simplifies to

$$\phi = e^{i\omega t} \sum_{m=0}^{\infty} \frac{C_{v_m}}{\sin \pi v_m} \left(a_{v_m} \cos v_m \theta + \sin v_m \theta \right) \left[J_{v_m}(kr) J'_{-v_m}(kR_1) - J_{-v_m}(kr) J'_{v_m}(kR_1) \right] \quad (1.22)$$

The expression in the square bracket is the characteristic function of wave motion in curved ducts. For simplicity it will be denoted $F_{\nu}(r, R_1)$ or in an abbreviated form F_{ν} . Its derivative with respect to the argument of Bessel functions, for the inner curved wall, that is, at R_1 , is always equal to zero. On the outside curved wall, at R_2 , F_{ν} is zero for all characteristic values ν_m . To determine values of constants C_{ν_m} we differentiate equation (1.22) with respect to θ and require that, at $\theta = 0$, the tangential vibrational velocity of particles be equal to the velocity of the vibrating piston $v_0 e^{i\omega t}$

$$\left. \frac{1}{r} \frac{\partial \phi}{\partial \theta} \right|_{\theta=0} = \sum_{m=0}^{\infty} \frac{1}{r} \frac{C_m \nu_m}{\sin(\pi \nu_m)} \left[J_{\nu_m}(kr) J'_{\nu_m}(kR_1) - J_{-\nu_m}(kr) J'_{-\nu_m}(kR_1) \right] = v_0 \quad (1.23)$$

where, to simplify the notation, C_m is written for C_{ν_m} .

To be able to write an expression for C_m we have to use the orthogonality conditions satisfied by the set $F_{\nu_m} = \left[J_{\nu_m}(kr) J'_{-\nu_m}(kR_1) - J_{-\nu_m}(kr) J'_{\nu_m}(kR_1) \right]$, as given in appendix 2.

The result is

$$\frac{C_m}{\sin(\pi \nu_m)} = \frac{v_0 e^{i\omega t} \int_{R_1}^{R_2} F_{\nu_m} dr}{\nu_m \int_{R_1}^{R_2} \frac{1}{r} F_{\nu_m}^2 dr} \quad (1.24)$$

The integral $\int_{R_1}^{R_2} \frac{1}{r} F_{\nu_m}^2$ is easily reducible to a sum of integrable expressions of which one vanishes. The evaluation of this integral is given in appendix 3.

The result is

$$\int_{R_1}^{R_2} \frac{1}{r} F_{\nu_m}^2 dr = \frac{r F'_{\nu_m}}{2\nu_m} F'(\nu) \Big|_{R_1}^{R_2} \quad (1.25)$$

where $F(\nu) = \frac{\partial F_{\nu_m}}{\partial \nu_m}$ and ' indicates differentiation with respect

to the argument of $F(\nu)$. The integral $\int_{R_1}^{R_2} \nu_0 F_{\nu_m}$ dr, for $\nu_0 =$

constant, can be integrated using the following expansion in Bessel functions, as given in "Handbook of Mathematical Functions". (32)

$$\int_{R_1}^{R_2} J_{\nu}(kr) dr = \frac{2}{k} \left[J_{\nu+1} + J_{\nu+3} + \dots \right] \Big|_{R_2} - \frac{2}{k} \left[J_{\nu+1} + J_{\nu+3} + \dots \right] \Big|_{R_1}$$

The sums of Bessel functions of increasing order $\pm \nu_m + 1$, $\pm \nu_m + 3, \dots$ in complex numbers, converge rapidly and the two first terms should give a satisfactory solution.

Summing up, the final expression for the velocity potential is

$$\phi = \sum_{m=0}^{\infty} \left(\frac{C_m}{\sin(\pi v_m)} \sin v_m \theta + \frac{D_m}{\sin(\pi v_m)} \cos v_m \theta \right) \left[J_{v_m}(kr) J'_{-v_m}(kR_1) - J_{-v_m}(kr) J'_{v_m}(kR_1) \right] \quad (1.26)$$

where

$$v_0 = \sqrt{\frac{2 \frac{a^2 - 1}{\ln a}}{4(kR_1)^{-2} + a^2 + 1 + \frac{a^2 - 1}{\ln a}}} \quad (1.20)$$

$$v_m = i \left\{ \frac{\frac{m\pi}{\ln a} - \frac{(kR_1)^2 (a^2 - 1) \left[2 + \frac{m^2 \pi^2}{(\ln a)^2} \right]}{4m\pi \left(1 + \frac{m^2 \pi^2}{(\ln a)^2} \right)}} \right\} \quad (1.17)$$

$m = 1, 2, 3, \dots$

In equation (1.26) only D_m , proportional to a_{v_m} in equation (1.5), remains undetermined.

1.3 Typical Physical Systems

The constants D_m must be determined by the remaining boundary conditions. These conditions depend on the configuration of the system under consideration.

1.30 Infinite bend. - Suppose an infinitely long circular duct for which the closest physical example is a tightly wound coil of which the pitch is negligible compared to the radius of curvature of the duct. The far end boundary condition for an infinite duct is that no reflection of waves must be considered.

To determine D_m in equation (1.26) we rewrite $(C_m \sin v_m \theta + D_m \cos v_m \theta)$, which is a convenient expression for study of standing waves, into a form better suited for study of propagation of waves. An alternate form of the solution for $\frac{\theta''}{\theta} = -v_m^2$ is $C'_m e^{iv_m \theta} + D'_m e^{-iv_m \theta}$. The two coefficients C'_m and D'_m are not known, but may be obtained in terms of C_m and D_m . Equating the two expressions

$$\frac{1}{\sin(\pi v_m)} \left[+\frac{1}{2} (iC_m + D_m) e^{iv_m \theta} + \frac{1}{2} (-iC_m + D_m) e^{+iv_m \theta} \right]$$

where D_m is the unknown to be determined.

The new, alternate, expression for the velocity potential is

$$\phi = \sum_{m=0}^{\infty} e^{i\omega t} \frac{1}{2} \left[(iC_m + D_m) e^{-iv_m \theta} + (-iC_m + D_m) e^{iv_m \theta} \right] \frac{F_{v_m}}{\sin(\pi v_m)} \quad (1.27)$$

where F_{v_m} is the radius depending term of the velocity potential, the characteristic function of the problem.

Let us consider the imaginary roots $v_m = i\mu_m$, with $\mu_m > 0$, ($m = 1, 2, 3, \dots$). We have now:

$$\phi = \sum_{m=1}^{\infty} e^{i\omega t} \frac{1}{2} \left[(iC_m + D_m) e^{\mu_m \theta} + (-iC_m + D_m) e^{-\mu_m \theta} \right] \frac{F_{v_m}}{\sin(\pi v_m)}$$

As $\theta \rightarrow \infty$, to avoid values which increase without limit with increasing values of θ we must set

$$-iC_m = D_m$$

and

$$\phi_m = \sum_{m=1}^{\infty} -e^{i\omega t} \frac{iC_m}{\sin(\pi v_m)} e^{-\mu_m \theta} F_{v_m} = \sum_{m=1}^{\infty} e^{i\omega t} \frac{D_m}{\sin(\pi v_m)} e^{-\mu_m \theta} F_{v_m} \quad (1.28)$$

which represents attenuated vibration of a compressible, inviscid fluid. Solutions pertaining to the imaginary roots vanish shortly after the inlet to the duct. The solution given by the real root v_0 is

$$\phi_0 = e^{i\omega t} \frac{1}{2} \left[(iC_0 + D_0) e^{-iv_0 \theta} + (-iC_0 + D_0) e^{iv_0 \theta} \right] \frac{F_{v_0}}{\sin(\pi v_0)}$$

To eliminate the waves going into the negative direction of θ , we put $iC_0 = D_0$ and obtain

$$\phi_0 = \frac{iC_0 F_{v_0}}{\sin(\pi v_0)} e^{i(\omega t - v_0 \theta)} = \frac{D_0 F_{v_0}}{\sin(\pi v_0)} e^{i(\omega t - v_0 \theta)} \quad (1.29)$$

which is a wave equation representing free and undamped oscillations of a compressible, inviscid fluid.

Adding the obtained solutions the velocity potential of infinitesimal waves in an infinite two-dimensional curved duct is

$$\phi(r, \theta, t) = \frac{D_0 F_{v_0}}{\sin(\pi v_0)} e^{i(\omega t - v_0 \theta)} + \sum_{m=1}^{\infty} e^{i\omega t} \frac{D_m F_{v_m}}{\sin(\pi v_m)} e^{-\mu_m \theta} \quad (1.30)$$

The amplitude of the moving wave is given by the constant and by the characteristic function $F_{v_0}(r, R_1)$ of the first term of the

equation (1.30). The exponential function $\exp i(\omega t - \nu_0 \theta)$ describes the harmonic motion. The second term of this equation represents the decaying oscillations. The amplitude of these oscillations depends on the radius. Basically, the motion in curved bends is characterized by non-plane oscillations. The detailed evaluation of these waves and oscillations will give the degree of this non-uniformity.

The harmonic function $\exp i(\omega t - \nu_0 \theta)$ depends on the characteristic value ν_0 (eq. (1.20)) which is the wave number of motion when expressed in cylindrical coordinates. It has been named by Krasnushkin⁽⁸⁾ "angular wave number"; ν_0 is a nondimensional, real and fractional number.

The propagation of waves in a curved duct is profoundly influenced by the boundary conditions (i.e., by the curvature of the duct). Consider $\exp i(\omega t - \nu_0 \theta)$ where ω is proportional to the forcing frequency of the piston and the phase velocity $\dot{\theta} = \omega/\nu_0$. The exponential function may be written $\exp i(\omega t - \nu_0 s/r)$ where $s = r\theta$ is the arc length. The wave constant on every circular path is

$$k' = \frac{\nu_0}{r} = \frac{2\pi}{\lambda(r)} \quad \text{and so} \quad \lambda(r) = \frac{2\pi r}{\nu_0} \quad \text{and} \quad \dot{s} = \frac{\omega r}{\nu_0}$$

where \dot{s} is the apparent phase velocity on a circle. In a curved duct the wave length and the apparent phase velocity are proportional to radius. The theory shows that, in the duct, there is an infinite set of simple waves of one frequency but of varying wave length.

It may be shown that for the case of a slightly bent duct the developed equations for wave propagation in bends are, in the limit, exactly those for a straight duct as demonstrated by Rayleigh. This will verify the result of the present analysis. Equation (1.20)

$$v_0 = \sqrt{\frac{2 \frac{a^2 - 1}{\ln a}}{4(kR_1)^{-2} + 1 + a^2 + \frac{a^2 - 1}{\ln a} - (a^2 - 1) \ln a}}$$

for $a \rightarrow 1$, with $\lim_{a \rightarrow 1} \frac{a^2 - 1}{\ln a} = 2$ and with $(kR_1) \ll 1$

$$\text{gives } v_0 = \sqrt{\frac{1}{(kR_1)^{-2} + 1}} \approx kR_1$$

while the apparent phase velocity on a circle becomes $\dot{s} = \frac{\omega r}{v_0} \rightarrow$

$\frac{\omega r}{kR_1} \rightarrow \frac{\omega}{k} = c$, the velocity of sound in unbounded space.

The angular wave number for short waves obtained by Buchholz⁽⁷⁾ and Rice⁽¹⁴⁾ does not meet this condition. Using our nomenclature they have

$$v_0 = \sqrt{(kR_1)^2 a + \frac{1}{4} + \frac{3}{2} \frac{(kR_1)^2 (a - 1)^2}{\pi^2} + F(a - 1)}$$

which for $a \rightarrow 1$ tends to $v_0 \approx \sqrt{(kR_1)^2 + \frac{1}{4}}$

The expression for angular wave number obtained by Grigor'yan⁽⁹⁾ is

$$v_0 = a(kR_1) \sqrt{\frac{3a - 1}{5a - 3}}$$

It tends to $v_0 = (kR_1)$ for $a \rightarrow 1$, as required. However, for

$a > 1$ its value does not agree with equation (1.20). In view of the fact that Grigor'yan uses an approximate solution (expansion in Taylor series) while equation (1.20) is a characteristic value of an exact solution, a verification of the solution at the lower limit and a progressive deficiency at the higher values of the variable are quite possible.

1.31 Straight infinite duct. - In order to satisfy the equation of motion in a bend followed by a straight duct we will match the solution given by equation (1.26) with

$$\phi = \sum_{n=-\infty}^{\infty} E_n e^{i(\omega t + \xi_n x + \zeta_n y)} \quad (1.31)$$

which represents an aggregate of plane waves in a straight tube, x being measured along the axis of the tube, y is perpendicular to it and $y = 0$ is at the center of the tube. The coefficients ξ_n and ζ_n are to be determined.

The Helmholtz equation in Cartesian coordinates reads

$$\frac{\partial^2 \phi}{\partial x^2} + \frac{\partial^2 \phi}{\partial y^2} + k^2 \phi = 0 \quad (1.32)$$

Differentiating equation (1.31) and substituting into the Helmholtz equation we obtain

$$-\xi_n^2 - \zeta_n^2 + k^2 = 0$$

or

$$\xi_n^2 = k^2 - \zeta_n^2$$

Rewriting equation (1.31)

$$\phi = \sum_{n=-\infty}^{\infty} \left(E_n' e^{+ix\sqrt{k^2-\zeta_n^2}} + E_n'' e^{-ix\sqrt{k^2-\zeta_n^2}} \right) e^{i(\zeta_n y + \omega t)}$$

or more generally

$$\begin{aligned} \phi = \sum_{n=-\infty}^{\infty} e^{i\omega t} & \left\{ e^{ix\sqrt{k^2-\zeta_n^2}} \left[P_n e^{i\zeta_n y} + Q_n e^{-i\zeta_n y} \right] \right. \\ & \left. + e^{-ix\sqrt{k^2-\zeta_n^2}} \left[P_n' e^{i\zeta_n y} + Q_n' e^{-i\zeta_n y} \right] \right\} \end{aligned} \quad (1.33)$$

Equation (1.33) represents waves going in the positive and the negative directions of x and y . Differentiating with respect to y and applying, at limits $y = \pm L$, the boundary condition of perfectly rigid wall, we have

$$P_n e^{i\zeta_n L} - Q_n e^{-i\zeta_n L} = 0$$

$$P_n e^{-i\zeta_n L} - Q_n e^{+i\zeta_n L} = 0$$

and similar homogeneous system for P_n' and Q_n' .

The consistency condition is

$$e^{2iL} - e^{-2iL} = 0$$

which gives

$$\sin 2\zeta_n L = 0$$

$$2\zeta_n L = n\pi \quad \zeta_n = \frac{n\pi}{2L}$$

$$n = 0, 1, 2, 3, \dots$$

(1.34)

Noting that

$$k = \frac{\omega}{c} = \frac{2\pi}{\lambda}$$

$$\zeta_n = \frac{n\pi}{2L} > \frac{\pi}{2L} > \frac{2\pi}{\lambda} = k$$

$$n = 1, 2, 3 \tag{1.35}$$

λ being assumed much greater than L .

Substituting the values of P_n, P'_n and Q_n, Q'_n from the compatibility equations into equation (1.33) we have

$$\phi = e^{-i\omega t} \sum_{n=0}^{\infty} \cos \left[\zeta_n (y + L) \right] \left(E'_n e^{ix \sqrt{k^2 - \zeta_n^2}} + E''_n e^{-ix \sqrt{k^2 - \zeta_n^2}} \right)$$

and, writing out explicitly the solution for $n=0$

$$\phi = e^{i\omega t} \left\{ E'_0 e^{ikx} + E''_0 e^{-ikx} + \sum_{n=1}^{\infty} \cos \left[\zeta_n (y + L) \right] \left[E'_n e^{-x \sqrt{\zeta_n^2 - k^2}} + E''_n e^{x \sqrt{\zeta_n^2 - k^2}} \right] \right\}$$

If we now assume the straight tube to be infinite we must eliminate the exponentials with positive powers of x . With $E'_0 = E''_0 = 0$ we obtain .

$$\phi = e^{i\omega t} \left\{ E_0 e^{-ikx} + \sum_{n=1}^{\infty} E_n \cos \left[\zeta_n (y + L) \right] e^{-x \sqrt{\zeta_n^2 - k^2}} \right\} \tag{1.36}$$

which is the final form of the equation of motion in the straight duct. The first term on the right hand side of this equation

represents a plane wave. The second term is an infinite set of attenuated vibrations. Differentiating equation (1.36) with respect to y will give expression for transverse vibrations. When differentiated, the first, permanent term yield no component. Therefore, only the set of higher modes produces attenuated transverse oscillations. This result discloses that the considered long waves in a straight duct must be plane to propagate.

Based on the above then, a general incident long wave will produce a traveling wave and attenuated transient components. This condition will remain until the initial wave straightens out and the transverse components diminish to zero. The initial wave then travels as a plane wave of reduced amplitude.

1.32 θ_2 radians bend followed by a straight infinite duct.- To analyze the motion in the system bend-straight duct, it is necessary to determine the D_m (in the equation of motion in the bend) and the E_n (in the equation of motion in the straight tube) using relations

$$\frac{1}{r} \frac{\partial \phi}{\partial \theta} = \frac{\partial \phi}{\partial x} \quad \text{and} \quad \frac{\partial \phi}{\partial r} = \frac{\partial \phi}{\partial y} \quad \text{at} \quad \begin{cases} \theta = \theta_2 \\ x = 0 \end{cases} \quad (1.37)$$

that is, the continuity conditions at the junction bend-straight tube. The velocity components, with

$$L = \frac{R_2 - R_1}{2} \quad \text{and} \quad y = r - \frac{R_1 + R_2}{2}, \quad \text{are:}$$

$$\frac{1}{r} \frac{\partial \phi}{\partial \theta} = e^{i\omega t} \left\{ \frac{C_0}{\sin(\pi\nu_0)} \frac{\nu_0}{r} F_{\nu_0} e^{-i\nu_0\theta} + \sum_{m=1}^{\infty} \frac{\nu_m}{r} \frac{F_{\nu_m}}{\sin(\pi\nu_m)} \left[C_m \cos \nu_m \theta - D_m \sin \nu_m \theta \right] \right\}$$

$$\frac{\partial \phi}{\partial x} = e^{i\omega t} \left\{ -ikE_0 e^{-ikx} - \sum_{n=1}^{\infty} \sqrt{\zeta_n^2 - k^2} E_n \cos \left[\zeta_n (r - R_1) \right] e^{-x \sqrt{\zeta_n^2 - k^2}} \right\}$$

$$\frac{\partial \phi}{\partial r} = e^{i\omega t} \left\{ \frac{iC_0}{\sin(\pi\nu_0)} F'_{\nu_0} e^{-i\nu_0\theta} + \sum_{m=1}^{\infty} \frac{F'_{\nu_m}}{\sin(\pi\nu_m)} \left[C_m \sin \nu_m \theta + D_m \cos \nu_m \theta \right] \right\}$$

$$\frac{\partial \phi}{\partial y} = e^{i\omega t} \left\{ - \sum_{n=1}^{\infty} \zeta_n E_n \left[\sin \zeta_n (r - R_1) \right] e^{-x \sqrt{\zeta_n^2 - k^2}} \right\}$$

37

Equations (3.10) at $\theta = \theta_2$ and $x = 0$ are

$$\frac{C_0}{\sin(\pi\nu_0)} \frac{\nu_0}{r} F_{\nu_0} e^{-i\nu_0\theta_2} + \sum_{m=1}^{\infty} \frac{\nu_m}{r} F_{\nu_m} \left[\frac{C_m \cos \nu_m \theta_2 - D_m \sin \nu_m \theta_2}{\sin(\pi\nu_m)} \right] = -ikE_0 - \sum_{n=1}^{\infty} \sqrt{\zeta_n^2 - k^2} E_n \cos \left[\zeta_n (r - R_1) \right] \quad (1.38)$$

$$\frac{iC_0}{\sin(\pi\nu_0)} F'_{\nu_0} e^{-i\nu_0\theta_2} + \sum_{m=1}^{\infty} \frac{F'_{\nu_m}}{\sin(\pi\nu_m)} \left[C_m \sin \nu_m \theta_2 + D_m \cos \nu_m \theta_2 \right] = - \sum_{n=1}^{\infty} \zeta_n E_n \sin \left[\zeta_n (r - R_1) \right] \quad (1.39)$$

„Multiplying equation (1.38) by F_{ν_m} and using the orthogonality properties established earlier we obtain

$$D_m \sin v_m \theta_2 = C_m \cos v_m \theta_2$$

$$\begin{aligned}
 & \frac{ikE_0 \int_{R_1}^{R_2} F_{v_m} dr + \frac{C_0 v_0}{\sin(\pi v_0)} e^{-iv_0 \theta_2} \int_{R_1}^{R_2} \frac{F_{v_0} F_{v_m}}{r} dr + \sum_{n=1}^{\infty} E_n \sqrt{\zeta_n^2 - k^2} \int_{R_1}^{R_2} F_{v_m} \cos[\zeta_n(r - R_1)] dr}{\frac{v_m}{\sin(\pi v_m)} \int_{R_1}^{R_2} \frac{1}{r} F_{v_m}^2 dr} \\
 & \hspace{25em} (1.40)
 \end{aligned}$$

The integral in the denominator is given in the appendix 3. To calculate E_n we multiply equation (1.39) by $\sin[\zeta_n(r - R_1)]$ and by orthogonality of the sine functions

$$\begin{aligned}
 E_n = & \frac{-\frac{iC_0}{\sin(\pi v_0)} e^{-iv_0 \theta_2} \int_{R_1}^{R_2} F_{v_0}' \sin[\zeta_n(r - R_1)] dr + \sum_{m=1}^{\infty} [C_m \sin v_m \theta_2 + D_m \cos v_m \theta_2] \int_{R_1}^{R_2} \frac{F_{v_m}'}{\sin(\pi v_m)} [\sin \zeta_n(r - R_1)] dr}{\zeta_n \int_{R_1}^{R_2} \sin^2[\zeta_n(r - R_1)] dr} \\
 & \hspace{25em} (1.41)
 \end{aligned}$$

The denominator is directly integrable

$$\begin{aligned} \zeta_n \int_{R_1}^{R_2} \sin^2 \left[\zeta_n (r - R_1) \right] dr &= \int_0^{n\pi} \sin^2 \left[\zeta_n (r - R_1) \right] d(r - R_1) \\ &= \frac{1}{2} \zeta_n (r - R_1) \Big|_0^{n\pi} - \frac{1}{4} \sin 2 \left[\zeta_n (r - R_1) \right] \Big|_0^{n\pi} = \frac{n\pi}{2} \end{aligned} \quad (1.42)$$

Rearranging and substituting equation (1.41) into equation (1.40) we will get the desired expression for D_m .

Besides D_m the only unknown in the above expressions is E_o . It will be obtained by integrations of equation (1.38). The last term is identically zero and there remains

$$-ikE_o \int_{R_1}^{R_2} dr = \frac{C_o v_o}{\sin(\pi v_o)} e^{-1v_o \theta_2} \int_{R_1}^{R_2} \frac{F v_o}{r} dr + \sum_{m=1}^{\infty} \int_{R_1}^{R_2} \frac{v_m}{r} \frac{F v_m}{\sin(\pi v_m)} \left[C_m \cos(v_m \theta_2) - D_m \sin(v_m \theta_2) \right] dr \quad (1.43)$$

The integral $\int_{R_1}^{R_2} \frac{F_{\nu m}}{r} dr$ is not directly obtainable. Let us consider the Bessel equation

$$F'' + \frac{1}{r} F' + \left(k^2 - \frac{\nu^2}{r^2}\right) F = 0$$

Multiplying by r and integrating (with $rF' \Big|_{R_1}^{R_2} = 0$)

$$k^2 \int_{R_1}^{R_2} r F_{\nu m}' dr = \nu^2 \int_{R_1}^{R_2} \frac{F_{\nu m}}{r} dr$$

An integral $\int_0^R r F_{\nu m}' dr$ can be evaluated by a general formula

$$\int_0^z t^\mu J_\nu(t) dt = z^{\mu+1} \sum_{k=0}^{\infty} \frac{(-1)^k (z/2)^{\nu+2k}}{K! (\nu+k+1)(\mu+\nu+2k+1)} \quad \text{Re}(\mu+\nu) > -1$$

The integral

$$\int_{R_1}^{R_2} F_{\nu m}' \sin \left[\zeta_n (r - R_1) \right] dr$$

will reduce, by integration by parts, to the integral

$$-\zeta_n \int_{R_1}^{R_2} F_{\nu m} \cos \left[\zeta_n (r - R_1) \right] dr \quad (1.44)$$

which is already present in the equation (1.40).

The evaluation of integral

$$\int_{R_1}^{R_2} F_{v_m} \cos \zeta_n (r - R_1) dr \quad (1.45)$$

is relegated to appendix 4.

The form of the solutions and of the expressions for the constants obtained so far are too complex to allow detail conclusions. However, equation (1.30) which defines the potential in an infinite bend indicates that there will be both a steady field of transmitted velocities and a decaying field. Furthermore there will be a field of standing radial vibrations throughout the bend. Similarly, equation (1.36) for the straight duct shows that there will be both the transmitted and the decaying velocity fields in the duct and that the radial oscillations exist only at the inlet. You will note that these equations do not permit the evaluation of the amplitude and distribution of the oscillations. However, expanding the functions and integrations will simplify the algebraic expressions and result in numerical data. The alternating series, described by the summation terms, converge very rapidly and will yield accurate data that will allow a physical interpretation of results.

2.0 INTEGRATED SOLUTION

Before any numerical application of the derived equation is considered it is worthwhile to analyze the functions present in the final expression for the velocity potential

$$\phi = \sum_{m=0}^{\infty} \frac{e^{i\omega t}}{\sin(\pi\nu_m)} \left(C_m \nu_m \sin \nu_m \theta + D_m \cos \nu_m \theta \right) \left[J_{\nu_m}(kr) J'_{-\nu_m}(kR_1) - J_{-\nu_m}(kr) J'_{\nu_m}(kR_1) \right] \quad (1.26)$$

The discussion will begin by an analysis of the Bessel functions, followed by an analysis of

$$F_{\nu_m}(r) = J_{\nu_m}(kr) J'_{-\nu_m}(kR_1) - J_{-\nu_m}(kr) J'_{\nu_m}(kR_1)$$

evaluation of coefficients C_m , D_m and coefficients E_n for the two typical duct systems to be concluded by interpretation of the final equations of motion.

2.1 The Characteristic Functions F_{ν_m} and Coefficients C_m

2.10 The real root solution. - Let us consider the solution of F_{ν_0}

in equation (1.26) pertaining to the real root ν_0 . Using the series expansions for $J_{\nu_0}(kr)$, $J_{-\nu_0}(kr)$ and for $J'_{\nu_0}(kr)$ and $J'_{-\nu_0}(kr)$ as given by equations (1.12) we obtain:

$$\begin{aligned}
 F_{\nu_0}(r, R_1) &= \frac{\sin(\pi \nu_0)}{4(kR_1)^{\nu_0} \pi (1 - \nu_0^2)} \cdot x \cdot \\
 &\left[\left(\frac{r}{R_1} \right)^{\nu_0} \left(-4\nu_0 + 4\nu_0^3 - 2(kR_1)^2 + \nu_0^2(kR_1)^2 - \nu_0(kR_1)^2 \right) \right. \\
 &\quad + \left(\frac{r}{R_1} \right)^{\nu_0} (kr)^2 \left(\nu_0 - \nu_0^2 + (kR_1)^2/2 - \nu_0(kR_1)^2/4 \right) \\
 &\quad + \left(\frac{r}{R_1} \right)^{-\nu_0} \left(-4\nu_0 + 4\nu_0^3 + 2(kR_1)^2 - \nu_0^2(kR_1)^2 - \nu_0(kR_1)^2 \right) \\
 &\quad \left. + \left(\frac{r}{R_1} \right)^{-\nu_0} (kr)^2 \left(\nu_0 + \nu_0^2 - (kR_1)^2/2 - \nu_0(kR_1)^2/4 \right) \right] \quad (2.1)
 \end{aligned}$$

In an direct application of this equation, we would neglect terms containing the second powers of (kr) and (kR_1) which are small of the fourth order. However, neglecting terms in $(kr)^2$ would restrict the characteristic function to constants and terms with logarithms of r . Consequently, to maintain generality we will keep the terms in $(kr)^2$ during analysis.

Using power series for the exponential functions

$$\left(\frac{r}{R_1}\right)^{\pm v_0} = 1 \pm v_0 \ln \frac{r}{R_1} + \frac{v_0^2 \left(\ln \frac{r}{R_1}\right)^2}{2!} \pm \frac{v_0^3 \left(\ln \frac{r}{R_1}\right)^3}{3!} + \dots$$

and neglecting terms in v_0^4 and terms containing products $(kr)^2$ $(kR_1)^2$ which are of the same order, we obtain

$$F_{v_0}(r, R_1) = \frac{\sin(\pi v_0)}{4\pi(kR_1)(1 - v_0^2)} \times$$

$$\left\{ \left[-8 + 8v_0^2 - 2(kR_1)^2 - 4(kR_1)^2 \ln \frac{r}{R_1} + 2v_0^2(kR_1)^2 \ln \frac{r}{R_1} \right. \right.$$

$$\left. - 4v_0^2 \left(\ln \frac{r}{R_1}\right)^2 - v_0^2(kR_1)^2 \left(\ln \frac{r}{R_1}\right)^2 - \frac{2}{3} v_0^2(kR_1)^2 \left(\ln \frac{r}{R_1}\right)^3 \right]$$

$$\left. + (kr)^2 \left[2 - 2v_0^2 \ln \frac{r}{R_1} + v_0^2 \left(\ln \frac{r}{R_1}\right)^2 \right] \right\} \quad (2.2)$$

This general solution of the Bessel equation well verifies the differential equation in a very wide range of radii ratios. For $a = R_2/R_1$ from 1 to 4 the error is negligible. For $a = 10$ the error is approximately 1 percent.

This equation, if greatly simplified by elimination of products of small terms becomes

$$F_{v_0}(r, R_1) = \frac{\sin(\pi v_0)}{4\pi(kR_1)} \left[-8 + 8v_0^2 - 2(kR_1)^2 - 4v_0^2 \left(\ln \frac{r}{R_1}\right)^2 \right.$$

$$\left. + 2(kr)^2 - 4(kR_1)^2 \ln \frac{r}{R_1} \right] \quad (2.3)$$

Equation (2.3), when applied to the differential equation, still yields a very satisfactory expression for v_0 at $r = R_2$ namely

$$v^2 \approx \frac{2 \frac{a^2 - 1}{\ln a}}{4(kR_1)^{-2}} = (kR_1)^2 \frac{a^2 - 1}{2 \ln a}$$

For numerical calculations F_{v_0} is, with high accuracy, equal to

$$F_{v_0} \approx - \frac{2 \sin(\pi v_0)}{\pi(kR_1)} \quad (2.4)$$

To obtain C_0 , we have, by equations (1.24) and (1.25), and using the expanded expression for F_{v_0}

$$C_0 = - \frac{v_0}{v_0} 2\pi(kR_1)(1 - v_0^2) \times$$

$$R_1 \frac{\left\{ \left[4 - (kR_1)^2 + 4v_0^2 \right] (a - 1) - (kR_1)^3 \frac{a^3 - 1}{3} + \left[2(kR_1)^2 - 4v_0^2 \right] a \ln a + 2v_0^2 a (\ln a)^2 \right\}}{\left[16 + 8(kR_1)^2 \right] \ln a + 4(kR_1)^2 (a^2 - 1) + 8(kR_1)^2 (\ln a)^2 + f(kR_1)^2 \cdot v_0^2}$$

which, if the small of the second and of the higher orders and neglected simplifies to

$$C_0 \approx -v_0 \frac{\pi(kR_1)}{2v_0} R_1 \frac{a - 1}{\ln a} \quad (2.5)$$

2.11 The imaginary roots solutions. - Let us consider the Bessel functions of pure imaginary order in the equation (1.26). Use will be made of expressions for the Bessel functions with real argument and of imaginary order and tables of functions which have been published by Buckens⁽²⁰⁾.

The very basic relations are

$$F_{\mu}(kr) + iG_{\mu}(kr) = 2^{i\mu} \Gamma(1 + i\mu) J_{i\mu}(kr) \quad (2.6)$$

where $i\mu = \nu$ and

$$G_{\mu}(kr) = A_{\mu}(kr) \sin [\mu \ln (kr)] + B_{\mu}(kr) \cos [\mu \ln (kr)]$$

$$F_{\mu}(kr) = A_{\mu}(kr) \cos [\mu \ln (kr)] - B_{\mu}(kr) \sin [\mu \ln (kr)]$$

The functions $A_{\mu}(kr)$ and $B_{\mu}(kr)$ are $A_{\mu}(kr) =$

$$\sum_{g=0}^{\infty} (\xi)_{2g} (ikr)^{2g} \quad B_{\mu} = \sum_{g=0}^{\infty} (\zeta)_{2g} (ikr)^{2g} \quad g = 0, 1, 2, 3, \dots \text{ and}$$

$$(\xi)_0 = 1, (\zeta)_0 = 0 \text{ and}$$

$$\zeta_{2g} = \frac{g\zeta_{2g-2} - \mu\xi_{2g-2}}{4g(\mu^2 + g^2)} \quad \xi_{2g} = \frac{g\xi_{2g-2} + \zeta_{2g-2}}{4g(\mu^2 + g^2)}$$

Neglecting the fourth and higher powers of (kr) we have

$$F_{\mu}(kr) = \left[1 - \frac{(kr)^2}{4(1 + \mu^2)} \right] \cos [\mu \ln(kr)] - \frac{(kr)^2}{4(1 + \mu^2)} \sin [\mu \ln(kr)]$$

$$G_{\mu}(kr) = \left[1 - \frac{(kr)^2}{4(1 + \mu^2)} \right] \sin [\mu \ln(kr)] + \frac{(kr)^2}{4(1 + \mu^2)} \cos [\mu \ln(kr)] \quad (2.7)$$

Substituting into equation (2.6) we obtain expressions for $J_{i\mu}(kr)$ and $J_{-i\mu}(kr)$ for $(kr) \ll 1$. In an abbreviated notation they are

$$F_{\mu}(kr) + iG_{\mu}(kr) = 2^{i\mu} \Gamma(1 + i\mu) J_{i\mu}(kr)$$

$$F_{\mu}(kr) - iG_{\mu}(kr) = 2^{-i\mu} \Gamma(1 - i\mu) J_{-i\mu}(kr)$$

The left hand sides of the above equations are complex conjugates.

Since

$$\overline{\Gamma(1 + i\mu)} = \overline{\Gamma(1 + i\mu)}$$

we conclude that $2^{i\mu} J_{-i\mu}(kr)$ is complex conjugate of $2^{-i\mu} J_{i\mu}(kr)$.

In equations (2.7), for $(kr) \ll 1$, terms in $(kr)^2$ may be neglected.

Expressions for $J_i(kr)$ and $J_{-i}(kr)$ simplify as follows

$$\cos [\mu \ln (kr)] + i \sin [\mu \ln (kr)] = 2^{i\mu} \Gamma(1 + i\mu) J_{i\mu}(kr) \quad (2.8a)$$

$$\cos [\mu \ln (kr)] - i \sin [\mu \ln (kr)] = 2^{i\mu} \Gamma(1 - i\mu) J_{-i\mu}(kr) \quad (2.8b)$$

Let us substitute into equation (2.8a) the value $\mu = m \frac{\pi}{\ln a}$

and consider the term $\sin [\mu \ln (kr)]$ for $kr = kR_1$ and $kr = kR_2$

We obtain

$$\sin \left[m\pi \frac{\ln kR_1}{\ln a} \right]$$

and

$$\sin \left[m\pi \frac{\ln kR_2}{\ln a} \right] = \sin \left[m\pi + m\pi \frac{\ln kR_1}{\ln a} \right]$$

The second expression is dephased by $m\pi$ with respect to the first one. We conclude that for $m = 1$, $[\mu = \pi/(\ln a)]$, $J_{i\mu}(kR_2)$ is the negative of $J_{i\mu}(kR_1)$ because it is reflection of $J_{i\mu}(kR_1)$ in the origin. For $m = 2$ $[\mu = 2\pi/(\ln a)]$, $J_{i\mu}(kR_2)$ will be numerically equal to $J_{i\mu}(kR_1)$ but will be rotated by 2π . The phase angle of the solutions for (kR_1) and (kR_2) by even and odd numbers of π implies that in the range of radii from R_1 to R_2 there will be a

number, increasing with m_i of pure imaginary or simply real $J_{i\mu}(kr)$.

Taking the derivative of the expression (2.6) with respect to the argument (kr) of the Bessel function we obtain

$$\begin{aligned} 2^{i\mu}\Gamma(1+i\mu)J'_{i\mu}(kr) &= \sin[\mu \ln(kr)] \left[2\zeta_2(kr) + \mu\xi_2(kr) - \frac{\mu}{(kr)} \right] \\ &+ \cos[\mu \ln(kr)] [\mu\zeta_2(kr) - 2\xi_2(kr)] \\ &+ i \left\{ -\cos[\mu \ln(kr)] \left[2\zeta_2(kr) + \mu\xi_2(kr) - \frac{\mu}{(kr)} \right] \right. \\ &\left. + \sin[\mu \ln(kr)] [\mu\zeta_2(kr) - 2\xi_2(kr)] \right\} \end{aligned}$$

All terms containing $\zeta_2(kr)$ and $\xi_2(kr)$ are small when compared with $\mu/(kr)$ and in the first approximation may be neglected.

The resulting equations are

$$2^{i\mu}\Gamma(1+i\mu)J'_{i\mu}(kr) = -\frac{\mu}{(kr)} \sin[\mu \ln(kr)] + i \frac{\mu}{(kr)} \cos[\mu \ln(kr)] \quad (2.9a)$$

$$2^{-i\mu}\Gamma(1-i\mu)J'_{-i\mu}(kr) = -\frac{\mu}{(kr)} \sin[\mu \ln(kr)] - i \frac{\mu}{(kr)} \cos[\mu \ln(kr)] \quad (2.9b)$$

By considerations identical to considerations applied to expressions (2.8) we conclude that the derivatives with respect to argument of the Bessel functions of pure imaginary order $J'_{-i\mu}(kr)$ and $J'_{i\mu}(kr)$, for $(kr) \ll 1$, are complex conjugates.

Using equations (2.8) and (2.9) we form $F_{\nu m}$ for $m \neq 0$

$$F_{\nu_m} = -2i \frac{\mu_m}{(kR_1)} \frac{\sin[\mu_m \ln(kr)] \sin[\mu_m \ln(kR_1)] + \cos[\mu_m \ln(kr)] \cos[\mu_m \ln(kR_1)]}{\Gamma(1 + i\mu_m) \Gamma(1 - i\mu_m)} \quad (2.10)$$

Since

$$\Gamma(1 + i\mu) \Gamma(1 - i\mu) = \frac{\pi\mu}{\sinh(\pi\mu)}$$

and using trigonometric transformation we have

$$F_{\nu_m} = i \frac{2 \sinh(\pi\mu_m)}{\pi(kR_1)} \cos \left[\mu_m \ln \frac{r}{R_1} \right] \quad (2.11)$$

Equation (2.11) shows that F_{ν_m} is a pure imaginary number and is a function of radius r . To check the degree of approximation used when neglecting terms in $(kr)^2$ we retrace our calculation and establish $F_{\nu_m}(r, R_1)$ with better accuracy. It is

$$F_{\nu_m} = i \frac{\sinh(\pi\mu_m)}{4(1 + \mu_m^2) \pi\mu_m (kR_1)} \times \left\{ -2\mu_m \left[4(1 + \mu_m^2) + (kR_1)^2 + (kr)^2 \right] \cos \left(\mu_m \ln \frac{r}{R_1} \right) + \left[4(kR_1)^2 + 2\mu_m^2 (kR_1)^2 - 2\mu_m^2 (kr)^2 \right] \sin \left(\mu_m \ln \frac{r}{R_1} \right) \right\}$$

Except for the first term in the expression of the cosine of the logarithm, all other terms are very small and are rapidly decreasing with increasing m . The simplified expression obtained by elimination of terms $(kr)^2$, which are small of the fourth order, retains

the character of the exact expression and may be considered as a very good approximation of the exact equation.

To calculate the constant C_m pertaining to the imaginary roots we evaluate the two integrals, $\int F_{v_m} dr$ and $\int \frac{1}{r} F_{v_m}^2 dr$, using equation (2.10) for F_{v_m} . This expression contains the variable r in functions $\sin[\mu \ln(kr)]$ and $\cos[\mu \ln(kr)]$. Before proceeding, we establish the necessary integrals starting with the well known integral

$$\int \sin(\ln r) dr = \frac{1}{2} r \sin(\ln r) - \frac{1}{2} r \cos(\ln r)$$

They are

$$\begin{aligned} \int r^p \sin(\mu \ln r) dr &= \frac{1}{[(p+1)^2 + \mu^2]} \left[(p+1)r^{(p+1)} \sin(\mu \ln r) \right. \\ &\quad \left. - \mu r^{(p+1)} \cos(\mu \ln r) \right] \\ \int r^p \cos(\mu \ln r) dr &= \frac{1}{[(p+1)^2 + \mu^2]} \left[\mu r^{(p+1)} \sin(\mu \ln r) \right. \\ &\quad \left. + (p+1)r^{(p+1)} \cos(\mu \ln r) \right] \end{aligned} \quad (2.12)$$

where p is unrestricted.

$$\int \frac{\sin^2(\mu \ln r)}{r} dr = \frac{1}{2} \ln r - \frac{1}{4\mu} \sin(2\mu \ln r) \quad (2.13)$$

$$\int \frac{\cos^2(\mu \ln r)}{r} dr = \frac{1}{2} \ln r + \frac{1}{4\mu} \sin(2\mu \ln r) \quad (2.14)$$

$$\int \frac{\sin(\mu \ln r) \cos(\mu \ln r)}{r} dr = -\frac{1}{4\mu} \cos(2\mu \ln r) \quad (2.15)$$

$$\int r \cos(\mu \ln r) \sin(\mu \ln r) dr = -\frac{r^2 \cos(2\mu \ln r)}{4\mu} + \frac{r^2}{4\mu[1 + \mu^2]} [\mu \sin(2\mu \ln r) + \cos(2\mu \ln r)] \quad (2.16)$$

$$\int r^2 \cos^2(\mu \ln r) dr = \frac{r^2 \sin(2\mu \ln r)}{4\mu} + \left(\frac{r}{2}\right)^2 - \frac{1}{\mu} \int r \sin(\mu \ln r) \cos(\mu \ln r) dr \quad (2.17)$$

The main lines of calculation of C_m are quite simple but lengthy. Omitting the algebraic intermediate steps, the result is

$$C_{m m}^v = -1 \frac{v_o \pi R_1(kR_1)}{4\mu_m \sinh(\pi\mu_m)} \times \frac{\left\{ -8\mu_m (a \cos m\pi - 1) - \frac{2(kR_1)^2}{1 + \mu_m^2} [2 + \mu_m + \mu_m^2] [a \cos m\pi - 1] + \frac{2(kR_1)^2}{3^2 + \mu_m^2} [\mu_m^3 - 3\mu_m] [a^3 \cos m\pi - 1] \right\}}{\left\{ (\mu_m^2 + 1) \ln a + 2(kR_1)^2 (a^2 - 1) \left[\frac{1}{1 + \mu_m^2} + \frac{1}{\mu_m^2} \left(1 - \frac{1}{1 + \mu_m^2} \right) \right] \right\}}$$

51

and retaining the large terms only

$$C_{m m}^v = i \frac{v_o \pi (kR_1) R_1}{\sinh(\mu_m \pi)} \frac{(a \cos(m\pi) - 1)}{\ln a (1 + \mu_m^2)} \quad (2.18)$$

and

$$C_m = \frac{v_o (kR_1) R_1}{m \sinh(\mu_m \pi)} \frac{(a \cos(m\pi) - 1)}{(1 + \mu_m^2)} \quad (2.19)$$

2.2 The Infinite Bend

2.20 Equations. - The integrated equation for the velocity potential $\phi(r, \theta, t)$ for an infinite bend may now be written directly by substitution of the derived expressions for C_0 , C_m and F_{v_0} , F_{v_m} into equation (1.30).

The velocity potential is

$$\begin{aligned} \phi = & -i \frac{v_0 R_1}{2v_0} e^{i(\omega t - v_0 \theta)} \frac{a-1}{\ln a} \left[-2 + (kr)^2/2 + 2v_0^2 - 2(kR_1)^2 - (kR_1)^2 \ln \frac{r}{R_1} - v_0^2 \left(\ln \frac{r}{R_1} \right) \right] \\ & + \frac{v_0 R_1}{4\pi} e^{i\omega t} \sum_{m=1}^{\infty} e^{-\mu_m \theta} \frac{a \cos m\pi - 1}{m\mu_m (1 + \mu_m^2)^{3/2}} \left\{ -2\mu_m \left[4(1 + \mu_m^2) + (kR_1)^2 + (kr)^2 \right] \cos \left(\mu_m \ln \frac{r}{R_1} \right) \right. \\ & \left. + \left[4(kR_1)^2 + 2\mu_m^2 (kR_1)^2 - 2\mu_m^2 (kr)^2 \right] \sin \mu_m \left(\ln \frac{r}{R_1} \right) \right\} \end{aligned} \quad (2.20)$$

and without terms small of the second order

$$\begin{aligned} \phi(r, \theta, t) = & i \frac{v_0}{v_0} R_1 \frac{a-1}{\ln a} e^{i(\omega t - v_0 \theta)} \\ & - 2 \frac{v_0 R_1}{\pi} e^{i\omega t} \sum_{m=1}^{\infty} \frac{a \cos(m\pi) - 1}{m(1 + \mu_m^2)} e^{-\mu_m \theta} \cos \left[\mu_m \ln \frac{r}{R_1} \right] \end{aligned} \quad (2.21)$$

The tangential vibrational velocity is

$$\begin{aligned}
 v(r, \theta, t) = & -e^{i\omega t} v_o \frac{R_1}{r} \frac{a-1}{2 \ln a} e^{i v_o \theta} \left[-2 + (kr)^2/2 + 2v_o^2 - 2(kR_1)^2 - (kR_1)^2 \ln \frac{r}{R_1} - v_o^2 \left(\ln \frac{r}{R_1} \right)^2 \right] \\
 & - \frac{v_o R_1}{4\pi r} e^{i\omega t} \sum_{m=1}^{\infty} e^{-\mu_m \theta} \frac{a \cos m\pi - 1}{m(1 + \mu_m^2)^2} \left\{ -2\mu_m \left[4(1 + \mu_m^2) + (kR_1)^2 + (kr)^2 \right] \cos \left(\mu_m \ln \frac{r}{R_1} \right) \right. \\
 & \left. + \left[4(kR_1)^2 + 2\mu_m^2 (kR_1)^2 - 2\mu_m^2 (kr)^2 \right] \sin \left(\mu_m \ln \frac{r}{R_1} \right) \right\} \quad (2.22)
 \end{aligned}$$

The radial vibrational velocity is

$$\begin{aligned}
 u(r, \theta, t) = & -i \frac{v_o R_1}{2v_o} e^{i(\omega t - v_o \theta)} \frac{a-1}{\ln a} \left[k^2 r - (kR_1)^2 / r - 2v_o^2 \ln \frac{r}{R_1} / r \right] \\
 & + e^{i\omega t} \frac{v_o R_1}{4\pi r} \sum_{m=1}^{\infty} e^{-\mu_m \theta} \frac{(a \cos(m\pi) - 1)}{m(1 + \mu_m^2)^2} \left\{ + 2\mu_m \left[4(1 + \mu_m^2) + (kR_1)^2 + (kr)^2 \right. \right. \\
 & \left. \left. - 4\mu_m^2 (kr)^2 \right] \sin \left(\mu_m \ln \frac{r}{R_1} \right) + \left[4(kR_1)^2 + 2\mu_m^2 (kR_1)^2 - 2\mu_m^2 (kr)^2 - 4(kr)^2 \right] \cos \left(\mu_m \ln \frac{r}{R_1} \right) \right\} \\
 & \quad (2.23)
 \end{aligned}$$

The real parts of these equations fully describe the propagation of acoustical waves in an infinite bend. To better visualize the dependence on radius of the final equations of motion, figure 2 shows $\cos \mu_m \ln(r)/(R_1)$ which appears in equations (2.22) and (2.23). This function is not very common. We note that the traced curves are shifted off-center due to the influence of the logarithm in the argument of the cosinus.

2.21 Discussion. - In the expression for the velocity potential the term which rapidly decreases, with increasing θ , is $\pi/2$ out of phase with respect to the other term which is a true wave of amplitude

$$\frac{v_o}{2v_o} R_1 \frac{a-1}{\ln a} \left[-2 + (kr)^2/2 + 2v_o^2 - 2(kR_1)^2 - (kR_1)^2 \ln \frac{r}{R_1} - v_o^2 \left(\ln \frac{r}{R_1} \right)^2 \right]$$

Since $kr \ll 1$, this amplitude is, in a first approximation, independent of radius and the progressive wave is nearly plane. The tangential vibrational velocity has both the permanent wave term and the attenuated vibration terms in phase. The permanent wave term is basically inversely proportional to the radius while the attenuated, disappearing term has a more involved radius dependence.

The radial vibrational velocities also have a permanent and an attenuated term. The permanent stationary vibrations are $\pi/2$ out of phase with the tangential components. The attenuated oscillations are in phase with the tangential velocities.

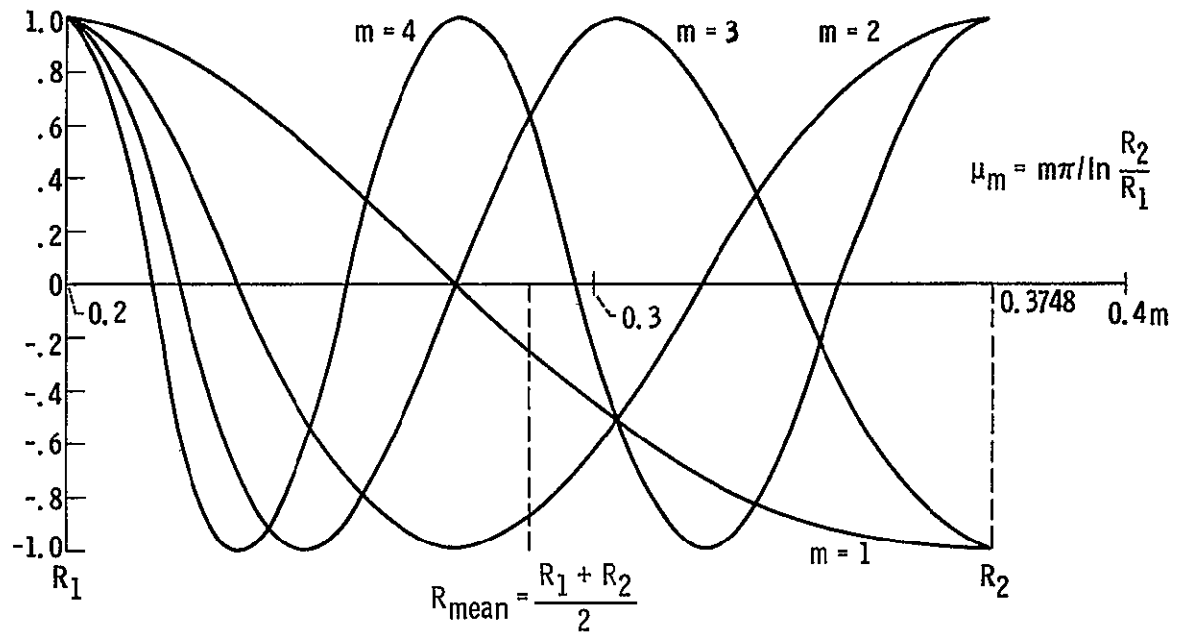


Figure 2. $-\text{Cos}[\mu_m \ln(r/R_1)]$ for $m = 1, 2, 3,$ and $4.$

A vectorial addition of the radial and tangential velocities yields motion's vibrational velocity and the direction of the wave front.

The propagation of waves in a curved duct is thus profoundly influenced by the curvature of the conduit. The amplitude of vibrational velocities is a function of both inner radius R_1 and of the radii ratio $a = R_2/R_1$. The tangential vibrational velocities are almost exactly inversely proportional to radius, that is, velocities follow the distribution of a potential vortex. The radial vibrational velocities are approximately two orders of magnitude smaller than the tangential velocities. Their radial distribution is governed by the three terms in the square bracket of the equation (2.23). The expressions derived for vibrational velocities in a bend permit a thorough discussion of the motion. The results obtained will be discussed with the aid of figures 3 to 8.

The tangential vibrational velocities of the propagating wave, as described by equation (2.22), very closely approximate a hyperbolic distribution across the channel's width. Figure 3 discloses that the vibrational velocities for $a = R_2/R_1$ up to 2.5 range from values close to $1.5v_0$ to approximately $0.5v_0$. It is noted that value of $v = v_0$ always falls on radii smaller than ducts centerline radius $R_m = (R_1 + R_2)/2$. For example, for $a = 2$, $v = v_0$ is at $r_{v=v_0}/R_1 \cong (a - 1)/\ln a = 1.4427$ while $R_m/R_1 = 1.5$. Performing the calculation for different values of the a , we obtain the relationship $r_{v=v_0}/R_m$ as a function of the parameter $a = R_2/R_1$.

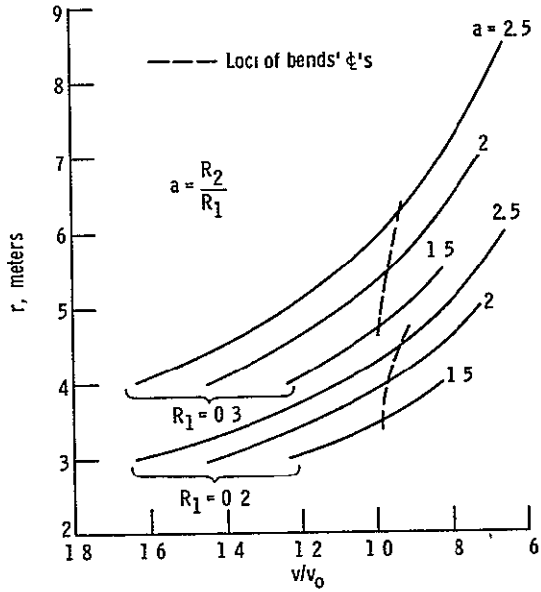


Figure 3 - Tangential vibrational velocities of the propagating long waves in curved ducts

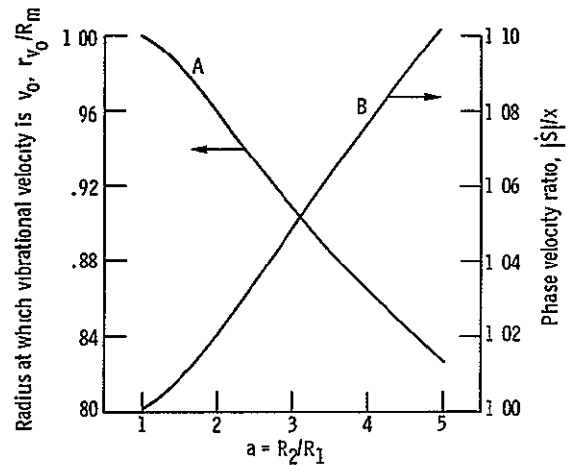


Figure 4' - Propagation of long waves in curved ducts. Curve A: Relation between the sharpness of the bend and the radial location of the average tangential velocity v_0 . Curve B: Comparison of the phase velocity in bends with phase velocity in straight ducts.

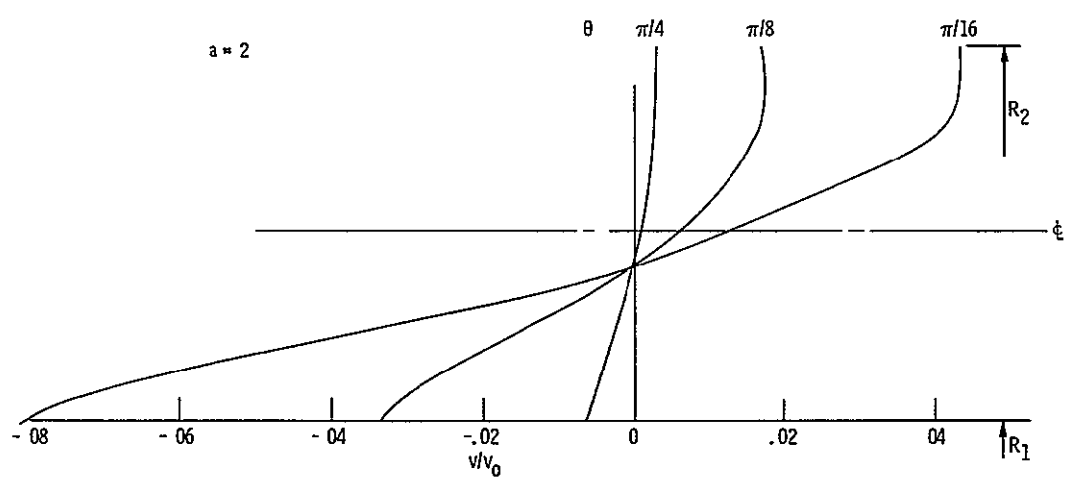


Figure 5 - Attenuated tangential vibrational velocities for three angular positions in a bend

This is shown in figure 4. The radius on which $v = v_0$ decreases proportionately to the increase in the sharpness of the bend.

The phase velocity of waves is also affected by bending of ducts. For a bend, the phase velocity is $\dot{\theta} = \omega/v_0$, as obtained from $(\omega t - v_0 \theta)$, while for a straight duct it is $\dot{x} = \omega/k$, as given by $(\omega t - kx)$. To compare the two velocities we average the tangential phase velocity, $\dot{\theta} r = \dot{s}$ over the duct width and obtain

$$|\dot{s}| = \frac{\omega}{v_0} R_m \quad \text{The ratio of the two velocities is } \frac{|\dot{s}|}{\dot{x}} = \frac{\omega}{c v_0} R_m = \frac{kR_m}{v_0}$$

This ratio is traced on figure 4. Clearly, the phase velocity in bends is always higher than in straight ducts. Furthermore it increases with increasing duct sharpness as measured by $a = R_2/R_1$. Therefore, if equal passage time in a straight and in a bend duct or phase equality are desired, the bend pipe must be made longer than the straight pipe.

The attenuated tangential vibrations which characterize change from motion of plane waves in straight duct to motion in a curved duct are examined in the next two figures. Figure 5 gives results of a sample calculation illustrating the behavior of those oscillations for a duct of radii ratio $a = 2$. The vibrations are basically of low amplitude. Even close to the piston, at $\theta = \pi/16$, they are one order of magnitude smaller than vibrations of the non-damped, propagating wave. The radial distribution of these oscillations changes significantly with wave angular position in the duct. At $\theta = \pi/4$ these oscillations are reduced to a very low level and are

nearly uniform across the width of the duct. Figure 6 shows the same oscillations calculated for three different duct widths but with a single angular position of $\theta = \pi/4$. The curve for $a = 2$ was taken directly from figure 5 for comparison purposes. The two other curves indicate that the decaying oscillations are much more pronounced and extend farther when induced in wider ducts.

The radial vibrational velocities, which characterize motion of waves in curved ducts, for long waves, are of low amplitude. The permanent, standing oscillations are shown in figure 7. They are calculated for duct radii ratios of 2, 3 and 4. Generally the amplitude of these oscillations is low, approximately two orders of magnitude smaller than the tangential velocities. The radial distribution is characterized by the lack of symmetry. The maxima of curves are shifted toward bend's inner wall.

This phenomenon is even more pronounced in the case of the non-propagating, damped, radial oscillations at the curved duct inlet. The amplitude and radial distribution of these oscillations is shown on figure 8 for three values of parameter a and at $\theta = \pi/4$. For $a = 2$ the permanent and the vanishing oscillations are of approximately the same amplitude. For $a = 3$ and 4 the decaying oscillations are about twice as large as the radial oscillation of the propagating wave. Therefore, the process of decay is much slower when ducts are wide.

The initial conditions, that is, the distribution of velocities on the vibrating piston, determined the type of the obtained solution.

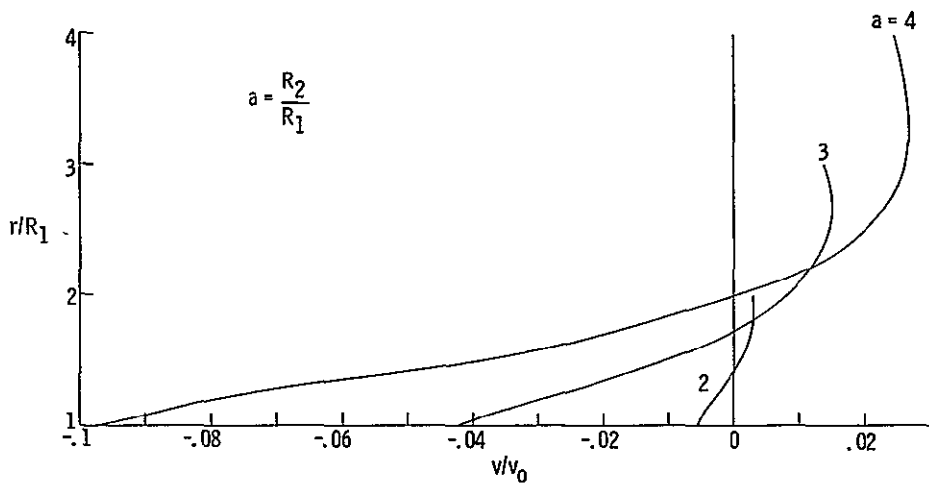


Figure 6. - Attenuated tangential vibrational velocities for three bends at $\theta = \pi/4$

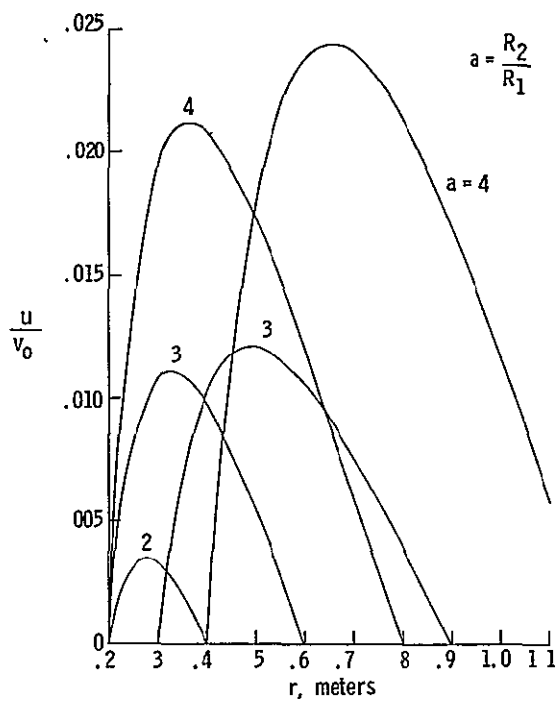


Figure 7. - Standing radial vibrational velocities in bends for three R_1 and three values of a

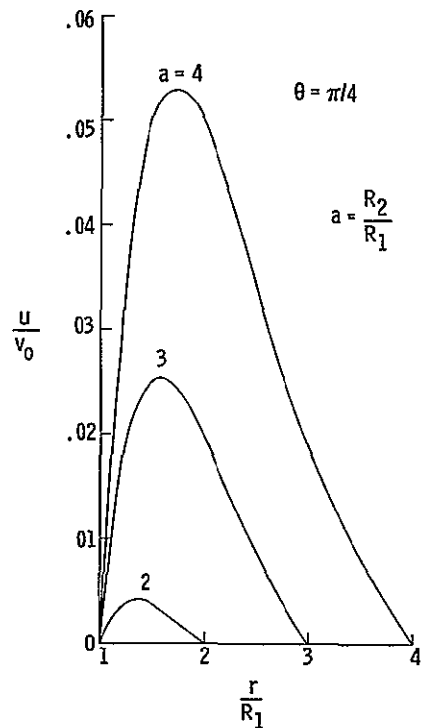


Figure 8. - Attenuated radial vibrational velocities at bend's inlet.

To verify the influence of the initial conditions let us compare the simple initial distributions in which the vibrational velocities at the piston will be independent, proportional and inversely proportional to the radius. Calculating the integral $\int v_o F_{v_m}(r) dr$ of the nominator of the constant C_m we obtain the following results

Initial Velocity Distribution	Amplitude of the Progressing Wave is Proportional to	Amplitude of the "m" th Decaying Wave is Proportional to
v_o	$\frac{a-1}{\ln a} + O(kr)^2$	$(a \cos m\pi - 1) + O(kr)^2$
$v_o \frac{r}{R_1}$	$\frac{a^2-1}{2 \ln a} + O(kr)^2$	$2 \frac{m^2\pi^2 + (\ln a)^2}{m^2\pi^2 + 4(\ln a)^2} (a^2 \cos m\pi - 1) + O(kr)^2$
$v_o \frac{R_1}{r}$	$1 + O(kr)^2$	zero + $O(kr)^2$

The first possibility, that is the particle vibrational velocity at the piston are independent of the radius, has been already discussed. The second possibility results in the amplitude of the wave and of the decaying vibrations strongly increasing with channel radii ratio a . The third possibility (potential vortex at the inlet) results in a wave of almost constant amplitude, independent of the parameter a and with vanishingly small damped oscillations at the inlet. The assumption that the tangential velocity at $\theta = 0$ be inversely proportional to the radius results in a remarkable simplification of the equation of motion because virtually only the undamped simple progressing and weak radial waves are present. Furthermore, the progressing waves are essentially independent of bend's radii ratio.

The physical meaning of the derived equations may now be discussed. We will make a direct parallel between solution of the Laplace equation $\nabla^2\phi = 0$ for inviscid, incompressible fluid and the Helmholtz equation $\nabla^2\phi + k^2\phi = 0$ for inviscid, compressible fluid. One of the solutions of the Laplace equation, written in cylindrical coordinates, gives the potential vortex. It is characterized by absence of radial velocities and, at every θ , the tangential velocity distribution is the same.

In the case of the Helmholtz equation with $v_0 = \text{const.}$ or proportional to the radius, equations indicate that long waves only gradually adjust themselves to the curvilinear boundaries until a permanent pattern of a free vortex type (in tangential vibrational velocities) is obtained on which vanishingly small components of linear and logarithmic nature are superimposed, and the previously discussed set of small radial oscillations is formed.

We conclude by saying that solution of the Helmholtz equation for a curved, two dimensional duct results almost exactly in a potential vortex in the tangential velocities with superimposed pattern of small standing radial oscillations. The presence of these radial vibrations distinguishes the Helmholtz equation from the Laplace equation type of motion.

2.3 θ_2 Radians Bend Followed by a Straight Infinite Duct

2.30 Motion in the bend. - To calculate the coefficients D_m which determine amplitude of vibrations near the outlet of a bend, we will proceed with integration of expressions established in the general

solution. Equations (1.40), (1.41) and (1.43) indicate that motion in a bend depends on the parameters of the straight duct that follows the bend. Obviously, motion in each segment of the ducting depends on motion in the entire system. The derived relationships are quite involved and simultaneous solution of these equations results in an infinite matrix in m and n . The coefficients D_m depend on coefficients C_m , E_o and E_n . However, by substitutions, it will be possible to express D_m in terms of known C_m only.

To simplify the writing the following symbols will be used.

For the integral of equation (1.45)

$$\int_{R_1}^{R_2} F_{v_m}(r) \cos \left[\zeta_n (r - R_1) \right] dr = A_{Fmn} \quad m \neq 0 \quad (2.24)$$

The coefficient E_o , as given by equation (1.43) is

$$E_o = i \frac{C_o v_o e^{-i v_o \theta_2}}{(k R_1)(a-1) \sin(\pi v_o)} \int \frac{F_{v_o}(r)}{r} dr$$

$$+ \frac{i}{(k R_1)(a-1)} \sum_{m=1}^{\infty} \frac{v_m C_m}{\sin(\pi v_m)} \left[\coth \mu_m \theta_2 + \frac{D_m}{i C_m} \right] \sinh(\mu_m \theta_2) \int \frac{F_{v_m}(r)}{r} dr \quad (2.25)$$

The first term, which will be designated by Z , consists of two parts. One large and independent of the parameters of the bend and a series of very small terms which are functions of R_1 and a .

The second term consists of a sum of very small terms only because

the main term of the integral $\int_{R_1}^{R_2} F_{v_m}(r)/r dr$ is

$$\int_{R_1}^{R_2} \frac{\cos \left[\mu_m \ln \frac{r}{R_1} \right]}{r} dr = 0$$

In an expanded form and with the help of simplifying symbols, equation (2.25) reads:

$$\begin{aligned} E_o = & Z + \chi_1 \left[\coth(\mu_1 \theta_2) - \tanh(\mu_1 \theta_2) \right] \\ & + \chi_2 \left[\coth(\mu_2 \theta_2) - \tanh(\mu_2 \theta_2) \right] + \dots \\ & + \chi_1 \beta_1 + \chi_2 \beta_2 + \dots \end{aligned} \quad (2.26)$$

$$\text{where } \beta_m = \left[\frac{D_m}{i C_m} + \tanh(\mu_m \theta_2) \right] \quad (2.27)$$

We note that for $\mu_m \theta_2$ larger than approximately 4, $\coth 4 \approx \tanh 4 \approx 1$. Typically for $\theta_2 = \pi/2$ and $a < 5$ this approximation is very satisfactory. In all practical applications of long wave motion in a 90° bend a simplified equation

$$E_o = i \frac{v_o}{k} e^{-i v_o \theta_2} \quad (2.28)$$

may be used with high accuracy. Equation (2.28) results from equation (2.26) when small terms of the second and higher orders are neglected.

By equations (1.40) and (1.41) a single expression for D_m may be obtained. It will be convenient to establish the ratio

(D_m/iC_m) rather than D_m alone. The relation is

$$\left(\frac{D_g}{iC_g}\right) = -\coth(\mu_g \theta_2) - \frac{ik E_0}{v_0 \sinh(\mu_g \theta_2)} - \frac{v_0 C_0 e^{-iv_0 \theta_2} \int \frac{F_{v_0} F_{v_m}}{r} dr}{v_0 \sinh(\mu_g \theta_2) \int F_{v_g} dr} - \frac{1}{v_0 \sinh(\mu_g \theta_2) \int F_{v_g} dr} \times$$

$$\left\{ \sum_{n=1}^{\infty} \sqrt{\zeta_n^2 - k^2} \Lambda_{Fgn} \left[-\frac{2}{n\pi} \frac{i C_0 e^{-iv_0 \theta_2}}{\sin(\pi v_0)} \int_{v_0} F'_{v_0}(r) \sin[\zeta_n(r - R_1)] dr \right] \right.$$

$$\left. + \sum_{n=1}^{\infty} \zeta_n \sqrt{\zeta_n^2 - k^2} \Lambda_{Fgn} \left[\frac{2}{n\pi} \sum_{m=1}^{\infty} \frac{i C_m}{\sin(\pi v_m)} \left[\sinh(\mu_m \theta_2) + \left(\frac{D_m}{i C_m}\right) \cosh(\mu_m \theta_2) \right] \Lambda_{Fmn} \right] \right\} \quad (2.29)$$

where E_0 is given by equation (2.26) and where D_g is the given particular D_m taken into consideration. Equation (2.29) cannot be simplified any further. It contains an infinite matrix in m and n because each D_g depends on all D_m and on the parameters of the straight duct. Expanding the matrix for $m = 1, 2, \dots$ and for $n = 1, 2, \dots$ and introducing the abbreviating symbols given by equations (2.26) and (2.27) we obtain

$$\begin{aligned}
\left(\frac{D_1}{i C_1}\right) &= -\coth(\mu_1 \theta_2) - \frac{v_0 C_0 \frac{e^{-i v_0 \theta_2}}{\sin(\pi v_0)} \int \frac{F'_{v_0} F'_{v_1}}{r} dr}{\sinh(\mu_1 \theta_2) v_0 \int F'_{v_1} dr} \\
&- \frac{ik}{v_0 \sinh(\mu_1 \theta_2)} \left[Z + \chi_1 \left(\beta_1 + \coth(\mu_1 \theta_2) - \tanh(\mu_1 \theta_2) \right) \right. \\
&\quad \left. \chi_1 \left(\beta_2 + \coth(\mu_2 \theta_2) - \tanh(\mu_2 \theta_2) \right) + \dots \right] \\
&- \frac{1}{\sinh(\mu_1 \theta_2) v_0 \int F'_{v_1} dr} \left[-\sqrt{\zeta_1^2 - k^2} \Lambda_{F11} \frac{2}{\pi} i \frac{C_0 e^{-i v_0 \theta_2}}{\sin(\pi v_0)} \int F'_{v_0} \sin[\zeta_1(r - R_1)] dr \right. \\
&\quad \left. - \sqrt{\zeta_2^2 - k^2} \Lambda_{F12} \frac{2}{2\pi} i \frac{C_0 e^{-i v_0 \theta_2}}{\sin(\pi v_0)} \int F'_{v_0} \sin[\zeta_2(r - R_1)] dr \right] \\
&- \dots
\end{aligned}$$

$$\begin{aligned}
& - \frac{1}{\sinh(\mu_1 \theta_2) v_0 \int_{v_1}^v dr} \left\{ \zeta_1 \sqrt{\zeta_1^2 - k^2} \Lambda_{F11} \frac{2}{\pi} \left[\beta_1 \frac{iC_1}{\sin(\pi v_1)} \cosh(\mu_1 \theta_2) \Lambda_{F11} \right. \right. \\
& \qquad \qquad \qquad + \beta_2 \frac{iC_2}{\sin(\pi v_2)} \cosh(\mu_2 \theta_2) \Lambda_{F21} \\
& \qquad \qquad \qquad + \dots \left. \right] \\
& \qquad \qquad \qquad + \zeta_2 \sqrt{\zeta_2^2 - k^2} \Lambda_{F12} \frac{2}{2\pi} \left[\beta_1 \frac{iC_1}{\sin(\pi v_1)} \cosh(\mu_1 \theta_2) \Lambda_{F12} \right. \\
& \qquad \qquad \qquad + \beta_2 \frac{iC_2}{\sin(\pi v_2)} \cosh(\mu_2 \theta_2) \Lambda_{F22} \\
& \qquad \qquad \qquad + \dots \left. \right] \left. \right\} \quad (2.30)
\end{aligned}$$

$$\left(\frac{D_2}{iC_2} \right) = - \coth(\mu_2 \theta_2) - \dots$$

Grouping, rearranging and adopting additional symbols to designate the constants of the matrix, we have

$$\begin{aligned}
\left[\beta_1 + \coth \mu_1 \theta_2 - \tanh \mu_1 \theta_2 \right] &= -A_1 - Z_1 - \sum_{n=1}^{\infty} Q_{1n} \\
&- \chi_{11} \left[\beta_1 + \coth (\mu_1 \theta_2) - \tanh (\mu_1 \theta_2) \right] \\
&- \chi_{12} \left[\beta_2 + \coth (\mu_2 \theta_2) - \tanh (\mu_2 \theta_2) \right] \\
&- \dots \\
&+ \eta_{11} \beta_1 + \eta_{21} \beta_2 + \eta_{31} \beta_3 + \dots
\end{aligned} \tag{2.31}$$

$$\begin{aligned}
\left[\beta_2 + \coth (\mu_2 \theta_2) - \tanh (\mu_2 \theta_2) \right] &= -A_2 - Z_2 - \sum_{n=1}^{\infty} Q_{2n} \\
&- \chi_1 \left[\beta_1 + \coth (\mu_1 \theta_2) - \tanh (\mu_1 \theta_2) \right] \\
&- \chi_2 \left[\beta_2 + \coth (\mu_2 \theta_2) - \tanh (\mu_2 \theta_2) \right] \\
&- \dots \\
&+ \eta_{12} \beta_1 + \eta_{22} \beta_2 + \eta_{32} \beta_3 + \dots
\end{aligned}$$

where A_m designates the second term in each row of equation (2.30), Z_m are used for products

$Z \frac{ik}{v_o \sinh(\mu_m \theta_2)}$ and Q_{mn} stand for terms in the third line of equations (2.30). The χ_{mn}

are χ_n multiplied by the factor in m in front of each square bracket and the η_{mn} are multipliers of all β_m in equation (2.30). Finally, by rearrangement, the matrix receives a symmetrical form.

$$\begin{aligned} & \left[\coth(\mu_1 \theta_2) - \tanh(\mu_1 \theta_2) \right] + A_1 + Z_1 + \sum_{n=1}^{\infty} Q_{1n} + \sum_{n=1}^{\infty} \chi_1 \left[\coth(\mu_1 \theta_2) - \tanh(\mu_1 \theta_2) \right] \\ & = \beta_1 (\eta_{11} - \chi_{11} - 1) + \beta_2 (\eta_{21} - \chi_{12}) + \beta_3 (\eta_{31} - \chi_{13}) + \dots \end{aligned} \tag{2.32a}$$

$$\begin{aligned} & \left[\coth(\mu_2 \theta_2) - \tanh(\mu_2 \theta_2) \right] + A_2 + Z_2 + \sum_{n=1}^{\infty} Q_{2n} + \sum_{n=1}^{\infty} \chi_2 \left[\coth(\mu_2 \theta_2) - \tanh(\mu_2 \theta_2) \right] \\ & = \beta_1 (\eta_{12} - \chi_{21}) + \beta_2 (\eta_{22} - \chi_{22} - 1) + \beta_3 (\eta_{32} - \chi_{23}) + \dots \end{aligned}$$

and similar expressions for the other rows of the matrix. The derived solution is very general. It applies to radii ratios of the bend in the range from 1 to 10; it has no limitations as to the length of the bend which may range from a small fraction of π to an infinite coil. This wide range of applicability was obtained by retaining in the solution, terms which are two orders of magnitude smaller than the principal terms. Now, reasonable limitations to this range of bend parameters will greatly simplify the final matrix. For bends with θ_2 greater than $\pi/4$

or $\pi/2$ and with $a < 2.2$ or $a < 5$ respectively, and neglecting small of the second order, the expressions in the square brackets drop out. Furthermore, the Z_m become Z and A_m , Q_{mn} and χ_{mn} tend to be negligibly small. The left side of each row of the matrix become a constant throughout the matrix and the right side further simplifies the matrix, equation (2.32a), reduces to

$$-2 = (\eta'_1 + 1)\beta'_1 + \eta'_{21}\beta'_2 - \eta'_{31}\beta'_3 - \dots \quad (2.32b)$$

$$-2 = \eta'_{12}\beta'_1 + (\eta'_{22} + 1)\beta'_2 - \eta'_{32}\beta'_3 - \dots$$

.

where "prime" on all variables indicate that they have been simplified by elimination of small of the second and higher orders. β'_m are now defined by

$$\left(\frac{D_m}{i C_m} \right) = -1 - \beta'_m \frac{e^{-i v_o \theta_2}}{e^{\mu_m \theta_2}}$$

This simplified form of the matrix which determines constants of motion in a bend is quite satisfactory for a wide range of applications.

With the expression for $\frac{D_m}{i C_m}$ already established and using the adopted abbreviating symbols, equation (1.41) for E_n is simply

$$E_p = -\frac{2}{p\pi} \left\{ \frac{i C_o e^{-i v_o \theta_2}}{\sin(\pi v_o)} \int F'_{v_o}(r) \sin[\zeta_p(r - R_1)] dr \right. \\ \left. - i \sum_{m=1}^{\infty} C_m \frac{\cosh(\mu_m \theta_2)}{\sin(\pi v_m)} \left[\tanh(\mu_m \theta_2) + \frac{D_m}{i C_m} \right] \zeta_n \Lambda_{Fmp} \right\} \quad (2.33)$$

where E_p is the given particular E_n taken into consideration.

Now equations for the velocity potential and the vibrational velocities are fully determined. However, expressions for ϕ , v and u respectively, cannot be written in a simple form because of use of series expansions of the Bessel functions and the involved expressions obtained for constants.

However, should we consider large terms only [neglecting small of the order of $(kR_1)^2$] and bends larger than $\pi/4$ so that

$$\sinh \mu\theta_2 \approx \cosh \mu\theta_2 \approx \frac{1}{2} e^{-\mu\theta_2}$$

we may form simple equations which with satisfactory accuracy describe the motion in curved ducts. In fact, these simplified equations make it possible to discuss several features of these relationships which would be otherwise obscured by large number of small terms which add to the exactness of the solution but not to the determination of the essential features of propagation except for the presence of the permanent radial standing vibrations. These vibrations, which characterize the motion of waves in bends, are described by terms small of the second order. Since these radial vibrations have been adequately discussed in connection with equation (2.23), there is no need to dwell on this subject again to any length.

The final approximate expressions for propagation of long waves in curved ducts will be based on equation (1.27) which may be written

as follows

$$\phi = \frac{iC_0 F_{v_0}}{\sin(\pi v_0)} e^{i(\omega t - v_0 \theta)} + e^{i\omega t} \sum_{m=1}^{\infty} \frac{1}{2} \frac{iC_m F_{v_m}}{\sin(\pi v_m)} \left[\left(1 + \frac{D}{iC_m}\right) e^{\mu_m \theta} + \left(-1 + \frac{D}{iC_m}\right) e^{-\mu_m \theta} \right]$$

Introducing the expressions for F_{v_0} , F_{v_m} and for $\left(\frac{D}{iC_m}\right)$ given respectively by equations (2.4), (2.11) and (2.32a), we obtain

$$\phi(r, \theta, t) = i \frac{v_0 R_1}{v_0} \frac{a-1}{\ln a} e^{i(\omega t - v_0 \theta)} + e^{i\omega t} \frac{v_0 R_1}{\pi} \sum_{m=1}^{\infty} \frac{a \cos(m\pi) - 1}{m(1 + \mu_m^2)} \cos \left[\mu_m \ln \frac{r}{R_1} \right] x \left[-2c^{-\mu_m \theta} + \beta_m e^{-v_0 \theta_2} \frac{(e^{\mu_m \theta} + e^{-\mu_m \theta})}{e^{\mu_m \theta_2}} \right] \quad (2.34)$$

where the term $e^{-i v_0 \theta_2}$ results from evaluation of E_n at $x = 0$ which is at $\theta = \theta_2$ and not at $\theta = 0$ and could be avoided should the coordinate θ of the bend be counted clockwise from the junction bend-straight duct.

Differentiating with respect to θ we obtain the tangential vibrational velocities

$$\begin{aligned}
v(r, \theta, t) = & v_0 \frac{R_1}{r} \frac{a-1}{\ln a} e^{i(\omega t - v_0 \theta)} + e^{i\omega t} 2v_0 \frac{R_1}{r} \sum_{m=1}^{\infty} \frac{a \cos(m\pi) - 1}{\ln a(1 + \mu_m^2)} \cos \left[\mu_m \ln \frac{r}{R_1} \right] e^{-\mu_m \theta} \\
& + e^{i(\omega t - v_0 \theta_2)} 2v_0 \frac{R_1}{r} \sum_{m=1}^{\infty} \frac{a \cos(m\pi) - 1}{\ln a(1 + \mu_m^2)} \frac{\beta_m}{2} \cos \left[\mu_m \ln \frac{r}{R_1} \right] \frac{(e^{\mu_m \theta} - e^{-\mu_m \theta})}{e^{\mu_m \theta_2}}
\end{aligned} \tag{2.35}$$

The first two terms of equation (2.35) are those of equation (2.22) of the wave motion in an infinite bend. The first term is a simple wave, the second the attenuated vibrations near the inlet section of the bend. The third term represents attenuated vibrations in the negative direction of θ , an adjustment of wave motion to discontinuity at the junction bend-straight duct. This term is identically zero at $\theta = 0$ and increases to a maximum at $\theta = \theta_2$. Because of the presence of $e^{-i v_0 \theta_2}$ these attenuated vibrations are in phase at θ_2 but out of phase of motion at $\theta < \theta_2$. Actually, this phase difference represents just time shift. We have $v_0 \theta_2 = \omega t_2$ where t_2 is time required for the wave to reach section θ_2 . Equation of motion in the straight duct have time counted from $t = 0$ at $x = 0$ or $\theta = \theta_2$ while actually the time count should have been started at a later time $t = t_2$.

The radial vibration velocities are obtained by differentiation with respect to radius

$$\begin{aligned}
 u(r, \theta, t) = & e^{i\omega t} 2v_0 \frac{R_1}{r} \sum_{m=1}^{\infty} \frac{a \cos(m\pi) - 1}{\ln a(1 + \mu_m^2)} \sin\left(\mu_m \ln \frac{r}{R_1}\right) e^{-\mu_m \theta} \\
 & - e^{i(\omega t - v_0 \theta_2)} 2v_0 \frac{R_1}{r} \sum_{m=1}^{\infty} \frac{a \cos(m\pi) - 1}{\ln a(1 - \mu_m^2)} \sin\left(\mu_m \ln \frac{r}{R_1}\right) \\
 & + \frac{\beta_m}{2} \left(\frac{e^{\mu_m \theta} - e^{-\mu_m \theta}}{e^{\mu_m \theta_2}} \right) \quad (2.36)
 \end{aligned}$$

This expression for radial vibrational velocities do not have any permanent wave term which was given by equation (2.23) when small of the second order were considered. The damped vibrations described by equation (2.36) exist near the inlet and near the outlet sections of the bend only although, theoretically, they extend over the whole propagation space. The amplitude of the inlet induced velocities is different than amplitude of exit induced velocities (factor 1 vs. $\beta/2$). Also the velocities near the inlet section are of opposite sign than velocities near the exit.

The motion in the straight duct may now be analysed. The coefficients E_n are given by equation (2.33). Substituting the established approximate values for $\frac{D}{iC_m}$ and C_m and simplifying we obtain

$$E_p = v_0 \frac{R_1}{\pi L} e^{-v_0 \theta_2} \sum_{m=1}^{\infty} \frac{a \cos(m\pi) - 1}{m(1 + \mu_m^2)} \Lambda_{mp} \beta_m \quad (2.37)$$

where Λ_{mp} are given by series and matrix in appendix 4, and β_m are numerical coefficients. Substituting equations (2.28) and (2.37) into equation (1.36), the velocity potential in the straight, infinite duct is approximately

$$\begin{aligned} \phi(y,x,t) = & e^{i(\omega t - v_0 \theta_2)} i \frac{v_0}{k} e^{-ikx} \\ & + \frac{2v_0 R_1}{\pi^2} \sum_{n=1}^{\infty} \frac{\zeta_n}{n} \cos \left[\zeta_n (y + L) \right] e^{-x \sqrt{\zeta_n^2 + k^2}} \\ & \times \sum_{m=1}^{\infty} \Lambda_{mn} \frac{a \cos(m\pi) - 1}{(1 + \mu_m^2)} \beta_m \end{aligned} \quad (2.38)$$

Differentiating with respect to x and simplifying, with

$\sqrt{\zeta_n^2 + k^2} \cong \zeta_n$, the axial vibrational velocities are

$$\begin{aligned} v(y,x,t) = & e^{i(\omega t - v_0 \theta_2)} v_0 e^{-ikx} - \frac{v_0 R_1}{2L^2} \sum_{n=1}^{\infty} n \cos \left[\zeta_n (y + L) \right] e^{-x \zeta_n} \\ & \times \sum_{m=1}^{\infty} \Lambda_{mn} \frac{a \cos(m\pi) - 1}{m(1 + \mu_m^2)} \beta_m \end{aligned} \quad (2.39)$$

The normal vibrational velocities are

$$\begin{aligned} u(y,x,t) = & -e^{i(\omega t - v_0 \theta_2)} \frac{v_0 R_1}{2L^2} \sum_{n=1}^{\infty} n \sin \left[\zeta_n (y + L) \right] e^{-x \zeta_n} \\ & \times \sum_{m=1}^{\infty} \Lambda_{mn} \frac{a \cos(m\pi) - 1}{m(1 + \mu_m^2)} \beta_m \end{aligned} \quad (2.40)$$

The double series in equations (2.39) and (2.40) are rapidly converging as long as x is not zero. The time shift coefficient $e^{-i v_0 \theta_2}$ is synchronizing the propagation of waves in the straight duct with wave motion in the bend.

3.0 ENERGY FLOW

Currently, no formulation of energy density or energy flow has been developed for long wave motion in bends. Karpman⁽⁸⁾ attempted to develop expressions for the kinetic and the potential energies of standing waves in a torus. However, because of mathematical difficulties he limited himself to partial results in terms of acoustic energy density which is sound energy per unit volume.

In systems with progressing waves it will be appropriate to evaluate energy flow or power per unit area, called sound intensity, which is given, in most general terms, by

$$I = \frac{1}{R_2 - R_1} \frac{1}{T} \int_0^T \int_{R_1}^{R_2} p \bar{v} \, dr \, dt$$

The \bar{v} designates the vector of the vibrational velocity normal to the wave front. The first integration, over the period of oscillation, is designed to replace instantaneous values with time averages. The second integration is necessary in the case of wave parameters dependent on radial coordinate to obtain an average over a cross section. The integration of the averaged product $p \bar{v}$ over a cross section is not necessary for plane waves in straight ducts but is necessary for plane waves in curved conduits.

Comparing sound intensity in a bend with sound intensity in a straight duct, will verify the derived equations of motion. To be successful, this comparison must involve the propagating waves only. To exclude the attenuated waves it will be assumed that in equations (1.30) and (1.36) the series with terms corresponding to $m = 1, 2, 3,$

... and to $n = 1, 2, 3 \dots$ are exactly zero. This will be very nearly true for sections of bends at angles close to $\pi/2$ or larger and for sections in straight ducts at length/width ratios of 2 or larger.

For the bend, the tangential vibrational velocity, as given by equation (2.22), for large θ and when time averaged is

$$\begin{aligned} \left| \bar{v}_\theta \right| &= \frac{v_o}{2} \frac{C_o}{\sin(\pi v_o)} \frac{F_{v_o}(r)}{r} \\ &= -v_o \frac{R_1}{r} \frac{a-1}{4 \ln a} \left[-2 + (kr)^2/2 + 2v_o^2 - 2(kR_1)^2 \right. \\ &\quad \left. - (kR_1)^2 \ln \frac{r}{R_1} - v^2 \left(\ln \frac{r}{R_1} \right)^2 \right] \end{aligned}$$

This velocity, when averaged over a cross section by integration is

$$\left| \bar{v} \right|_{\text{bend}} = v_o \left[1 - \delta_o(R_1, a) \right] \quad (3.1)$$

where δ_o is a small quantity of the second order. Equation (3.1) indicates that the kinetic energy of the tangential vibrations in the bend is less than the kinetic energy of the wave generated at the face of the piston. Some kinetic energy was transferred from the progressing wave into the standing radial oscillations.

Using the equations on page 37 and the relation (2.25) we obtain the tangential vibrational velocity in the straight duct, at a section of the duct remote from the junction with the bend.

$$\begin{aligned}
|\bar{v}|_{\text{straight}} &= -\frac{ik}{2} E_0 \\
&= \frac{k}{2} \frac{v_0 C_0}{(kR_1)(a-1) \sin(\pi v_0)} \int \frac{F_{v_0}}{r} dr \\
&\quad + \frac{k}{2(kR_1)(a-1)} \sum_{m=1}^{\infty} \frac{v_m C_m}{\sin(\pi v_m)} \times \left[\coth(\mu_m \theta_2) + \frac{D_m}{iC_m} \right] \\
&\quad \times \sinh(\mu_m \theta_2) \int \frac{F_{v_m}}{r} dr
\end{aligned}$$

Integrating this relationship over a cross section and averaging, yields the following relationship

$$\begin{aligned}
|\bar{v}|_{\text{straight}} &= \frac{v_0 C_0}{\sin(\pi v_0)} \int \frac{F_{v_0}}{r} dr + \sum_{m=1}^{\infty} \frac{v_m C_m}{\sin(\pi v_m)} \int \frac{F_{v_m}}{r} dr \times e^{-iv_0 \theta_2} \\
&= v_0 \left[1 - \delta_0(a, R_1) - \delta_m(v_m R, a, \theta_2) \right]
\end{aligned}$$

The kinetic energy transferred from the bend into the straight duct is further reduced by energy absorbed by standing radial vibrations near the junction of the bend and straight duct.

Like δ_0 , the "loss" δ_m for the long waves is also a small quantity, approximately three orders of magnitude smaller than the amplitude of the original wave.

For the bend the equation which describes pressure when time averaged, is as follows:

$$\begin{aligned}
|p| &= -\rho \left| \frac{\partial \phi}{\partial t} \right| = \frac{\rho \omega}{2} \frac{c_0}{\sin(\pi v_0)} F_{v_0}(r) \\
&= \frac{\rho \omega}{4} v_0 \frac{R_1(a-1)}{v_0^2 \ln a} \left[-2 + (kr)^2/2 + 2v_0^2 - 2(kR_1)^2 \right. \\
&\quad \left. - (kR_1)^2 \ln \frac{r}{R_1} - v_0^2 \left(\ln \frac{r}{R_1} \right)^2 \right]
\end{aligned}$$

In order to obtain an average value across a cross section, it is necessary to replace v_0 by kr and integrate the above equation. The equality of v_0 and kr was explained in detail in section 1.3. As you recall it simply indicates that motion in a bend consists of an infinite set of waves of different wavelength but of a single frequency. Therefore making the substitution and integrating results in the following expression.

$$|\bar{p}|_{\text{bend}} = \frac{\rho \omega}{k} v_0 \left[1 - \delta(a, R_1) \right]$$

In a straight duct, time averaged pressure is described by the expression

$$|\bar{p}|_{\text{straight}} = i \frac{\rho \omega}{2} E_0$$

It is noted that this expression parallels the expression for $|v|_{\text{straight}}$. Making the proper substitution and performing the integration, results in the following expression.

$$|\bar{p}|_{\text{straight}} = \frac{\rho \omega}{k} v_0 \left[1 - \delta_0(a, R_1) - \delta_m(v_m, a, R_1, \theta_2) \right]$$

Examining this expression we note that the potential energy of the progressing wave in the bend, and downstream from it, is also subject to a small decrease.

Finally, using the derived expressions, we can describe the flow of energy in the bend by the expression

$$I_{\text{bend}} = \frac{\rho\omega}{2k} v_o^2 \left[1 - \delta_o(a, R_1) \right]^2$$

and in the straight duct by the expression

$$I_{\text{straight}} = \frac{\rho\omega}{2k} v_o^2 \left[1 - \delta_o(a, R_1) - \delta_m(v_m, a, R_1, \theta_2) \right]^2$$

The long waves under consideration are subject to a loss of energy when going through a bend because some energy is retained in radial vibrations. However, at low frequencies, waves pass through bends very easily. This is because the reduction in the rate of flow of energy is very small.

A verification using the energy method of the approximate expressions, equations (2.21) and (2.38), may be made directly. We observe that the approximate expressions pertain to plane waves which are defined by

$$p = (\omega t - \bar{n} \cdot r)$$

where \bar{n} is a unit vector perpendicular to the wave front. For a plane wave the sound intensity vector \bar{i} is

$$\bar{i} = p\bar{v} = \rho c v^2 \bar{n} = \frac{p^2}{\rho c} \bar{n}$$

where the quantities p and v are already averaged over a period.

For the three expressions of the energy flow we have

$$pv = \rho \omega v_o^2 \frac{R_1^2}{v_o} \frac{(a-1)^2}{(\ln a)^2} \frac{1}{r}$$

$$\rho c v^2 = \rho c v_o^2 R_1^2 \frac{(a-1)^2}{(\ln c)^2} \cdot \frac{1}{r^2}$$

$$\frac{p^2}{\rho c} = \frac{\rho}{c} \omega^2 v_o^2 \frac{R_1^2}{v_o^2} \frac{(a-1)^2}{(\ln a)^2}$$

Equating

$$\frac{1}{r^2} = \frac{k}{v_o^2} = \frac{k}{v_o} \frac{1}{r}$$

which, as before, only requires substitution $k = v/r$ to verify the identity.

Finally, comparing the approximate expression for the straight duct and for the bend we have:

$$\text{for the straight duct} \quad i = \rho c \frac{|v_o|^2}{2}$$

where $|v_o|$ is averaged v_o over a period.

For the bend, averaging v_θ over cross section yields

$$\frac{1}{R_2 - R_1} \int_{R_1}^{R_2} v \, dr = \frac{1}{R_2 - R_1} v_o R_1 \frac{a-1}{\ln a} \int_{R_1}^{R_2} \frac{dr}{r} = v_o$$

$$\text{and } i_\theta = \rho c \frac{|v_o|^2}{2} \quad \text{and } i_{\text{bend}} = i_{\text{straight}}$$

which verifies the energy flow equations. This verification is based on approximate expressions in which small terms of the second and higher orders were neglected. However, the small terms describe

the radial oscillations that characterize the motion of waves in curved ducts. Since no consideration was given to energy which was transferred from the progressing wave to the standing radial oscillations, the energy flow in the straight duct equals the energy flow in the bend. This also equals the energy flow generated by the piston. There are no experimental data available to quantitatively verify these results. The reason is the physical difficulty of trying to examine the (very low) range of frequencies which is the subject of the present analysis. Usually the acoustics experimentation is carried out in the audible frequency range of 200 to 3000 Hz. Consequently only a qualitative verification is possible. This verification must be based on the extrapolation of the available experimental information to very low frequency range.

In 1955 Lippert⁽²⁵⁾ published data on characteristic transmission factor $T = B \exp i\beta$ of square and rounded 90° elbows. The amplitude B of the factor T is defined as ratio of sound pressure amplitudes of the transmitted wave at the output plane to the sound pressure amplitudes of the incident wave at the input plane. β is the phase angle of the transmitted wave with respect to the phase of the incident wave. As shown on figure 9, transmissivity of a 90° mitered bend is high at low frequencies (≤ 600 Hz) but close to 2200 Hz approaches zero. An experiment with a rounded 90° elbow indicates that rounding improved the transmissivity over the entire range of frequencies and eliminated the cut-off condition. The dotted line indicates extrapolation of Lippert's data. We conclude that at very

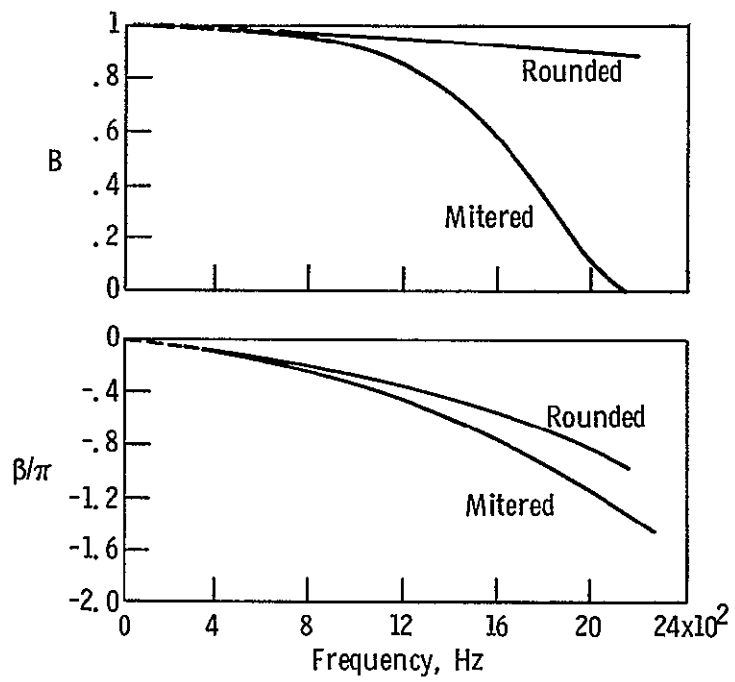


Figure 9. - Transmission of acoustic waves through 90° mitered and rounded elbows. Experimental data by Lippert⁽²⁵⁾.

low frequencies (1 to 10 Hz) the transmissivity of the two elbows is very high but not one-hundred percent. There will be some reflections and some transfer of energy from the progressing wave to the standing radial oscillations. At the limit, zero frequency, there is no wave motion and the potential flow of matter should suffer no losses of energy. That in effect is the case of a potential vortex. The lower curves on figure 9 show the phase change of the transmitted wave. The square mitered elbow and the rounded elbow produce similar phase changes, with virtually merging slopes at lower frequencies. Again, using extrapolation, we conclude that at low frequencies there will be some phase shift.

On the basis of these data, it may be concluded that results of this analytical study are qualitatively verified. The long waves penetrate and pass through bends easily. However there is some energy being stored in the bends which comes from the main wave. This stored energy is a very small, but not negligible.

4.0 NUMERICAL APPLICATION

The purpose of the numerical application is to obtain a solution for a conventional industrial setup which will give typical wave propagation pattern. At the same time it is intended to analyze the Bessel Functions of very small order and Bessel functions of pure imaginary order and real argument.

4.1 Selection of Parameters

In order to simplify the numerical calculations and to conform to the requirement that parameters must approximate a typical industrial installation we select the logarithm of the radii ratio, $\ln a$, such that μ_m , defined by,

$$v_m = i\mu_m = im \frac{\pi}{\ln a} \quad m = 1, 2, 3 \quad \text{be an integer}$$

Selecting $\ln a = 0.62831$ we obtain $\frac{\pi}{\ln a} = 5$, $v_m = im5$ and $a = R_2/R_1 = 1.8744$. This radii ratio is reasonable and approximates an industrial ducting.

To obtain the argument of the Bessel functions (kR_1) which will be a small, finite number, and a wave constant k and radius R_1 typical for industrial application we select

$$k = 0.1 \text{ m}^{-1}, R_1 = 0.2 \text{ m}$$

It follows that the wave length λ in free space, as defined by $\lambda = 2\pi/k$, is 62.28 m. With speed of sound in warm air of 350 m/sec, the frequency f is $f = kc/2\pi = 5.57$ cycles/sec and the corresponding rotational speed of a compressor generating those waves is 350 rpm which, again, is representative of industrial application. The argument of the Bessel functions will be, at the limits,

$$(kR_1) = 0.02 \quad \text{and} \quad (kR_2) = 0.03748$$

This argument is $\ll 1$ and the wave length is much larger than the dimension of the bend which satisfies the requirements of the theoretical treatment.

4.2 Bessel Functions and Characteristic Functions of the Problem

4.21 Solution pertaining to the real root. - Using the selected and calculated values of ν_0 and (kR_1) we have, by equation (1.20), the real root equal to

$$\nu_0 = 0.02828 \quad (4.1)$$

The evaluation of the Bessel functions of order ± 0.02828 for arguments (0.02), (0.03) and (0.037489) and of the derivative of Bessel functions of order ± 0.02828 for arguments $kR_1 = (0.02)$ and $kR_2 = (0.03748)$ is based on the expansion of $J_{\nu_0}(kr)$ in terms of increasing powers of the argument.

$$J_{\pm\nu_0}(kr) = \left(\frac{kr}{2}\right)^{\pm\nu_0} \left[\frac{1}{(\pm\nu_0)!} - \frac{(kr/2)^2}{(\pm\nu_0 + 1)!} + \frac{(kr/2)^4}{2(\pm\nu_0 + 2)!} + \dots \right]$$

and on the expansion of $J'_{\pm\nu_0}(kr)$ given by equation (1.12).

Because $(kr) \ll 1$ we may neglect the second and the following terms of the expansions. However, in order to evaluate the degree of approximation thus obtained we will keep the second term of the expansion. Since the expansions contain alternating terms, the error resulting from limiting expansion to a given term will be smaller than the first term which has been dropped.

Without entering into details of algebra the following numbers are obtained.

$$J_{v_0}(0.02) = 0.87789[1.015793 - 0.0000987] = 0.891667$$

$$J_{v_0}(0.03) = 0.888014[1.015793 - 0.0002222] = 0.9018412$$

$$J_{v_0}(0.03748) = 0.89361[1.015793 - 0.0003469] = 0.9074127$$

$$J_{-v_0}(0.02) = 1.13909[0.983158 - 0.0001012] = 1.119790$$

$$J_{-v_0}(0.03) = 1.126108[0.983158 - 0.0002276] = 1.106886$$

$$J_{-v_0}(0.03748) = 1.119056[0.983158 - 0.0003553] = 1.099811$$

These numbers are shown on figure 10.

Keeping only the first two terms of the expansions (1.12) we obtain

$$J'_{v_0}(0.02) = 1.25215$$

$$J'_{v_0}(0.03748) = 0.668134$$

$$J'_{-v_0}(0.02) = -1.59491$$

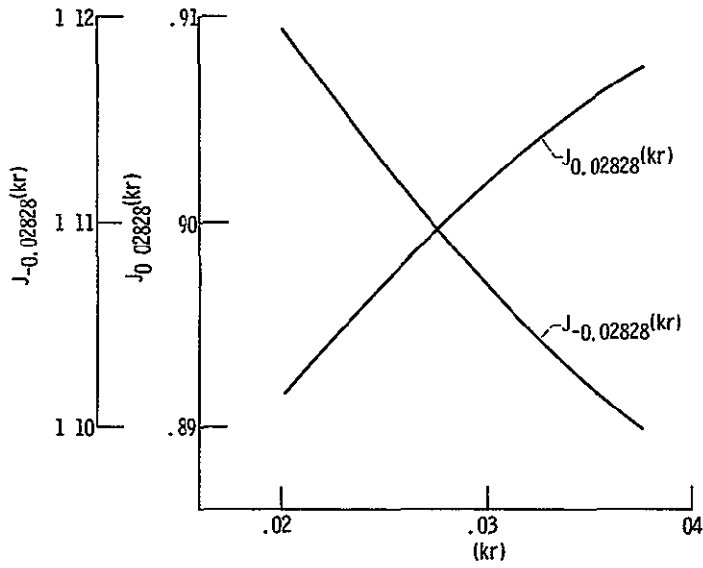
$$J'_{-v_0}(0.03748) = -0.851066$$

To check the results we substitute the values of the derivatives into equation (1.9)

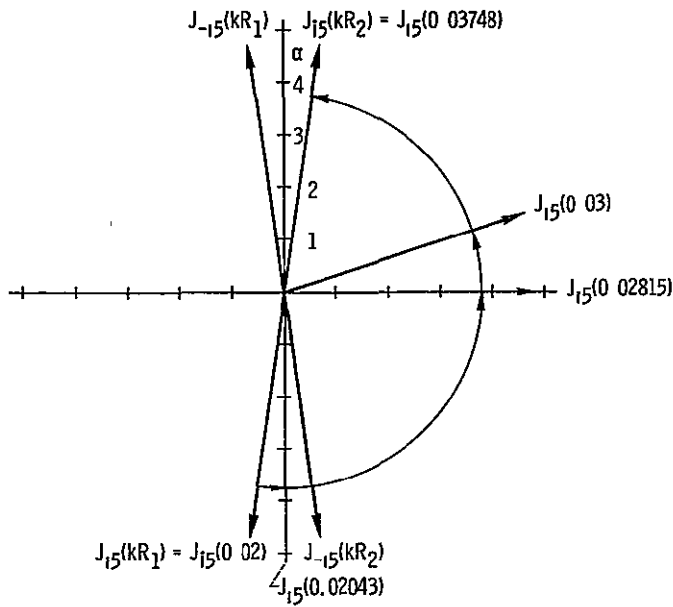
$$J'_{v_0}(kR_1)J'_{-v_0}(kR_2) - J'_{v_0}(kR_2)J'_{-v_0}(kR_1) = 0$$

The result is

$$-1.06566 + 1.06561 = -0.00005$$



(a) Bessel functions of order ± 0.02828 in the interval of the argument (kr) from 0.02 to 0.03748.



(b) Bessel functions of order $\pm i \left(m \nu \ln \frac{R_2}{R_1} \right) = \pm 15$ in the complex plane.

Figure 10. - Bessel functions of fractional and imaginary order.

Equation (1.9) is verified with an error of $\frac{0.00005}{1.0656} \times 100 = 0.001$ percent. For the three radii the value of $F_{v_0}(r)$ is

$$R_1 = 0.2 \quad F_{v_0} = -2.82420$$

$$r = 0.3 \quad F_{v_0} = -2.82434$$

$$R_2 = 0.3748 \quad F_{v_0} = -2.82437$$

with maximum variation of F_{v_0} over R_1 to R_2 of $\frac{0.00017}{2.824285} \times 100 = 0.006$ percent. This result indicates that the wave is very nearly plane. Using the equation (2.4) which was established without the second and following terms of expansion of $J_{\pm v}(kr)$ we obtain

$$F_{v_0} = -2.8240$$

The discrepancy between this value of F_{v_0} and the values calculated using the first and the second terms of this expansion is negligible, as assumed in the evaluation of the roots of the wave equation.

4.22 Solutions pertaining to the imaginary roots of the problems. -

To calculate the F_{v_m} pertaining to the imaginary roots, for $m = 1, 2, 3 \dots$, we start by evaluating the degree of approximation of our mathematical theory. The pure imaginary roots are given by equation (1.17) and only the first term of this equation was considered in analysis because the second term was assumed small.

Calculations confirm the theoretical development:

$$m = 1 \quad v_1 = i5 - i0.000083$$

$$m = 2 \quad v_2 = i10 - i0.000040$$

The second term is very small and decreases with increasing m .

To calculate the Bessel functions for v_m , $m = 1, 2, 3 \dots$, we calculate functions $G_\mu(kr)$, $F_\mu(kr)$ and $\Gamma(1 \pm i\mu)$ for different μ and (kr) .

We do not intend to go into details of the algebra. However, it may be worthwhile to show the technique of work and to give a sample calculation. We select

$$J_{v_1}(kR_1) = J_{i5}(0.02)$$

and propose to solve the equation (2.8a) with

$$\cos[5 \ln 0.02] = \cos[-19.5601] = 0.757997$$

$$\sin[5 \ln 0.02] = \sin[-19.5601] = -0.652258$$

Substituting

$$0.757997 - i0.652258 = 2^{i5} \Gamma(1 + i5) J_{i5}(0.02) \quad (4.2)$$

The left-hand side of the equation is a complex number whose modulus is $0.757997^2 + 0.652258^2 = 1$ and the argument is

$$2\pi - \operatorname{arctg} \frac{0.652258}{0.757997} = 5.57258. \quad \text{Substituting into (4.2) and taking}$$

$$\text{logarithm we have } i5.57258 = i3.4655 - 6.13032 + i3.815898 + \ln J_{i5}(0.02)$$

where

$$-6.13032 + i3.81898 = \ln \Gamma(1 + i5) \quad \text{as given by tables of functions, reference (32).}$$

Finally

$$6.13032 - i1.708818 = \ln J_{i5}(0.02)$$

or

$$459.6(\cos 1.708818 - i \sin 1.708818) = J_{i5}(0.02) \quad \text{and}$$

$$J_{i5}(0.02) = -63.236 - i455.229$$

Calculating the Bessel functions for arguments (0.03) and (kR_2) = 0.037489 we obtain

$$J'_{i5}(0.03) = 437.714 + i140.13$$

$$J'_{i5}(0.037489) = 63.236 + i455.229$$

The Bessel functions (as approximated by limited expansions) for the same three arguments but of negative order are complex conjugates of the above results. Calculating the derivatives of Bessel functions with respect to the argument, for arguments (kR_1)

0.02 and (kR_2) = 0.037489, we obtain

$$J'_{i5}(0.02) = 1.13807 \times 10^5 - i0.15805 \times 10^5$$

$$J'_{i5}(0.037489) = -6.0712 \times 10^4 + i0.843174 \times 10^4$$

and the same functions but of negative order are the complex conjugates of the above results. Again these conclusions are restricted to approximated expressions for the Bessel functions.

The calculated functions are shown on figure 10. On this figure we also indicated two particular values of $J_{i5}(kr)$ namely, the pure imaginary $J_{i5}(0.02043) = -i459.6$ and the real $J_{i5}(0.02815) = 459.6$. To check the calculated derivatives, we substitute the numerical values of the functions into equation (1.9). The results is

$$J'_{i5}(0.02)J'_{-i5}(0.037489) - J'_{i5}(0.037489)J'_{-i5}(0.02) = -i0.0231 \approx 0$$

The accumulated error equals 0.12 percent and may be tolerated.

4.3. The Two Physical Systems

The degree of accuracy of the derived basic functions has been established in the preceding section. The numerical application of

the integrated equations for the infinite coil and for the 90 degree bend followed by a straight infinite duct may now be done without going into details of the component functions.

4.31 Infinite coil. - The tangential and radial vibrational velocities are given by equations (2.22) and (2.23). The numerical application is straightforward. The alternating series in the two equations are converging rapidly as long as θ is not zero.

At $\theta = \pi/64, \pi/8$ and $\pi/4$ the seventh, the fifth, and the second term of the series, respectively, are already negligible. At $\theta = 3\pi/8$ the first terms of the series was smaller than 0.1 percent of the value of the simple wave term in equation (2.22).

At $\theta = 0$ the convergence is slow. Typically for $\theta = 0$ and at $r = R_1$ $v(R_1, 0, t) = v_0$

and

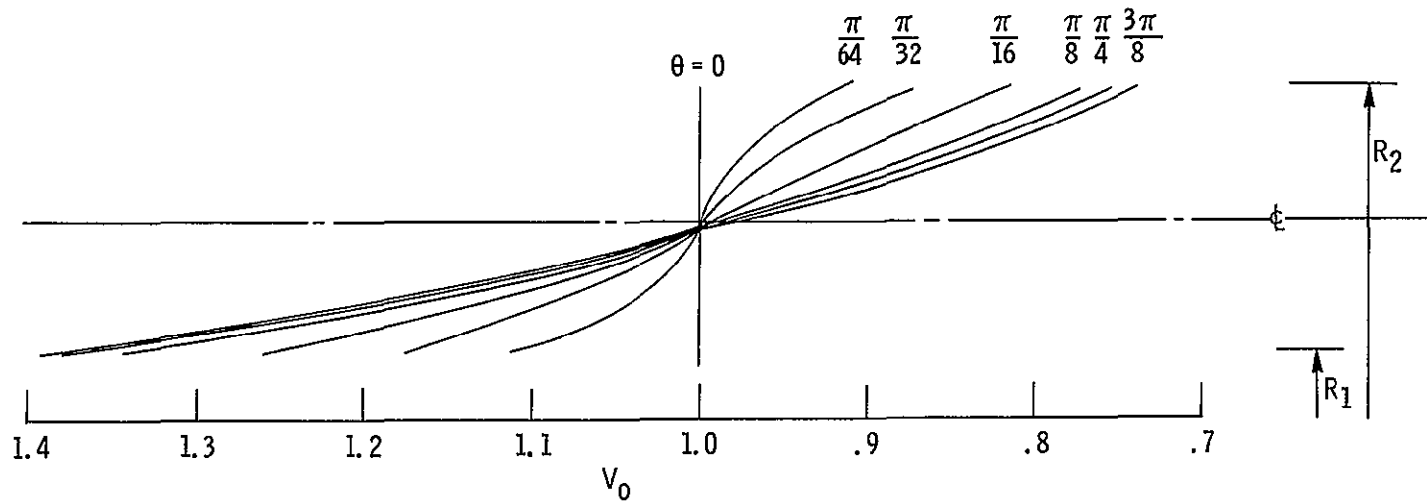
$$\frac{a-1}{\ln a} + 2 \sum_{m=1}^{\infty} \frac{a \cos(m\pi) - 1}{\ln a(1 + \mu_m^2)} = 1$$

and for $\theta = 0$ and $r = R_2$

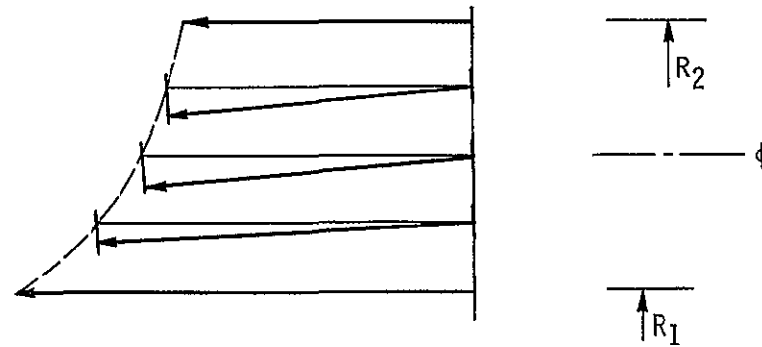
$$\frac{1}{a} \frac{a-1}{\ln a} + \frac{2}{a} \sum_{m=1}^{\infty} \frac{a - \cos(m\pi)}{\ln a(1 + \mu_m^2)} = 1$$

With 30 terms taken into consideration the error was still of the order of 1 percent. The calculated values of $v(r, \theta, t)$ are plotted on figure 11.

To better show the rapid velocity changes near the inlet section of the bend and the important final velocity dependence $(1/r)$ on the



(a) Tangential vibrational velocity distribution near inlet of an infinite coil.



(b) Magnitude and direction of vibrational velocities at section $\theta = \pi/16$.

Figure 11. - Infinite coil. Distribution of vibrational velocities.

radius, the calculated values are superposed. On the abscissa is the velocity magnitude in terms of v_0 .

About 25 percent of the velocity redistribution take place between $\theta = 0$ and $\pi/64$. By $\theta = \pi/8$ the distribution characteristic to potential vortex is nearly completed and changes become slow and it takes, from then on, an angle $\pi/4$ to reach the steady-state distribution.

The decaying radial vibrational velocities were calculated for one cross section, at $\theta = \pi/16$, and are compared with the permanent radial vibrations. The values are

Radius	Decaying $u(r, \pi/16, t)$	Permanent $u(r, \pi/16, t)$
R_1	0	0
$R_1 + (R_2 - R_1)/4$	$-0.0860 v_0$	$-0.002475 v_0$
$R_1 + (R_2 - R_1)/2$	$-0.0884 v_0$	$-0.002636 v_0$
$R_1 + 3(R_2 - R_1)/4$	$-0.0480 v_0$	$-0.001635 v_0$
R_2	0	0

The permanent radial oscillations are one order of magnitude smaller than the decaying oscillations at $\pi/16$. By vectorial addition, the magnitude and direction of vibrational velocities may be obtained.

For section $\theta = \pi/16$, figure 11 shows that the wave profile is not straight. It approximates in the vicinity of this section, a cosinus curve. Beyond section $\theta = 3\pi/8$ the radial velocities are so small that the wave profile is very nearly radial.

4.32 90 degree bend followed by a straight duct. - The wave pattern in a bend followed by a straight duct is much more involved than the wave propagation in an infinite coil. So is also the numerical application.

The problem of evaluation of integrals A_{mn} was already discussed and is reported in appendix 4. The evaluation of coefficients D_m or rather of the ratio (D_m/iC_m) , given by matrix (2.32a), was simplified, by elimination of small terms and reduced to matrix equation (2.32b) in β_m . This matrix, in principle infinite was, in the present numerical calculations, arbitrarily limited to six rows and columns. It is as follows:

$$2 = 1.9935 \beta_1' + \frac{0.73}{10^2} \beta_2' + \frac{0.3288}{10^2} \beta_3' + \frac{0.4015}{10^4} \beta_4' + \frac{0.7057}{10^5} \beta_5' + \frac{0.978}{10^5} \beta_6'$$

$$-2 = -0.208 \beta_1' - 2.001 \beta_2' - \frac{0.615}{10^2} \beta_3' + \frac{0.1286}{10^3} \beta_4' - \frac{0.1358}{10^4} \beta_5' + \frac{0.2743}{10^3} \beta_6'$$

$$-2 = -0.745 \beta_1' - \frac{0.4277}{10^2} \beta_2' - 2.000 \beta_3' - \frac{0.4887}{10^3} \beta_4' + \frac{0.141}{10^2} \beta_5' - \frac{0.786}{10^3} \beta_6'$$

$$-2 = -0.4128 \beta_1' + \frac{0.405}{2} \beta_2' - \frac{0.221}{10} \beta_3' - 1.995 \beta_4' - \frac{0.3837}{10} \beta_5' + \frac{0.178}{10} \beta_6'$$

$$-2 = -\frac{0.455}{10} \beta_1' - \frac{0.120}{10} \beta_2' + \frac{0.181}{10} \beta_3' - \frac{0.108}{10} \beta_4' - 1.9386 \beta_5' - \frac{0.314}{10} \beta_6'$$

$$-2 = -0.7615 \beta_1' + \frac{0.654}{10} \beta_2' - 0.2699 \beta_3' + 0.135 \beta_4' - 0.844 \beta_5' - 1.5768 \beta_6'$$

By inspection, we see that the first four β_m' 's will be close to unity. To have precise values, the matrix was solved by Cramer's rule on a digital computer. Furthermore, in order to ascertain that

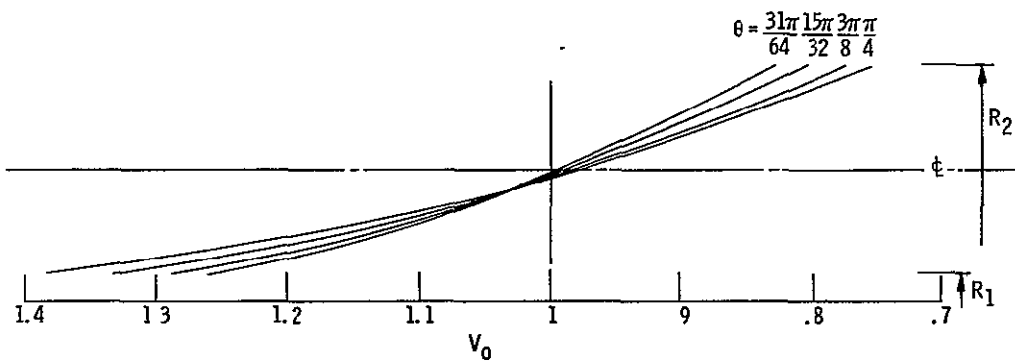
the arbitrary limitations of an infinite matrix to a square matrix 6x6 will not result in unrealistic values of β'_m 's, five computer runs were requested to obtain solutions of matrices 2x2, 3x3 and 6x6. The result is

Approximation	β'_1	β'_2	β'_3	β'_4	β'_5	β'_6
1st	1.00326					
2nd	0.99998	0.89374				
3rd	0.99896	0.89374	0.62598			
4th	0.99894	0.89379	0.62579	0.79069		
5th	0.99894	0.89378	0.62650	0.77137	1.00425	
6th	0.99893	0.89381	0.62640	0.77365	1.00024	0.24667

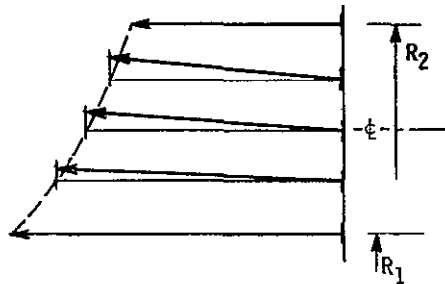
The variation of coefficients β'_m over the range of terms taken into consideration is negligible. Consequently, we assume that arbitrary limitation of the matrix to 6x6 is permissible. The values obtained by the sixth approximation will be used in calculations.

The calculation of the tangential and radial vibrational velocities [eqs. (2.35) and (2.36)] is direct. Figure 12 gives the results of the numerical application. At $\theta = 15\pi/32$ the distribution of tangential velocities is no more inversely proportional to radius. The wave is deformed, by significant, positive radial velocities. The series in the equations of motion are still limited, however, to one significant term only. At $\theta = 31\pi/64$, there are two significant terms in the series. We conclude that important changes in the values of vibrational velocities are confined to the last $\pi/32$ of the $\pi/2$ bend.

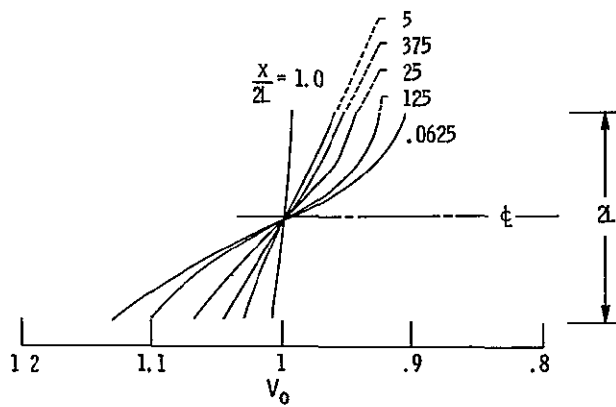
By the bend outlet the wave profile is no more radial. The effective vibrational velocity equal $\sqrt{v^2 + u^2}$ is in r positive



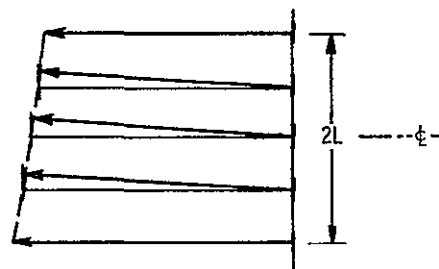
(a) Bend outlet. Distribution of tangential vibrational velocities.



(b) Vibrational velocities at section $\theta = 15\pi/32$.



(c) Straight duct inlet. Distribution of axial vibrational velocities.



(d) Vibrational velocities at $\frac{x}{2L} = 0.25$

Figure 12. - 90° Bend followed by a straight duct. Distribution of vibrational velocities.

direction, except at boundaries where it is tangential. This is also shown on figure 12. The direction of the effective vibrational velocities gives the wave front orientation.

The calculation of the vibrational velocities in the straight duct that follows the 90 degree bend is straightforward. Results of application of equations (2.39) and (2.40) are also reported on figure 12.

In the straight duct the waves are straightening out relatively fast. By $x/2L = 1$ there is already an almost straight wave similar to that which was generated at the bend inlet. Essentially, the process of straightening out of the wave is confined to the straight duct. Figure 13 shows that the tangential velocity $v = v_0$ remains in the bend in its equilibrium position at approximately $\cong R_1(a - 1)/\ln a$, which in this application, is at $r/R_1 = 1.392$, and only in the straight duct gradually bends closer to the center line of the duct. By $x/2L = 1.5$ the tangential vibrational velocity ($v_0 - \delta_0 - \delta_m$) is at the center line and, everywhere.

The verification of the simultaneous solution of the equations of motion for the bend and for the straight duct is shown on figure 14. The calculated tangential vibrational velocities for $r = R_1$ and $r = R_2$ for positions starting at the vibrating piston, through the bend and in the straight duct are taken from figures 11 and 12. The rapid changes in velocities by the bend exit are well illustrated. In spite of this, the values calculated for the bend match very well the values calculated for the straight duct. At $x/2L = 1$

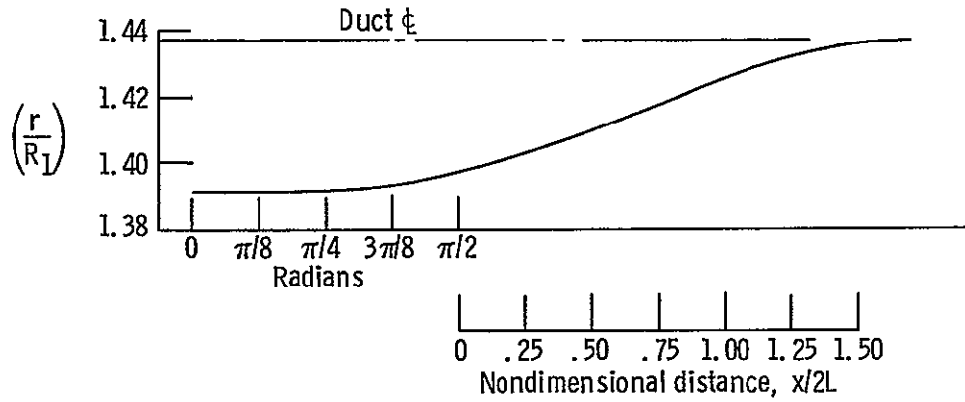


Figure 13. - Propagation in bend-straight duct system. Changes in location of the tangential vibrational velocity v_0 .

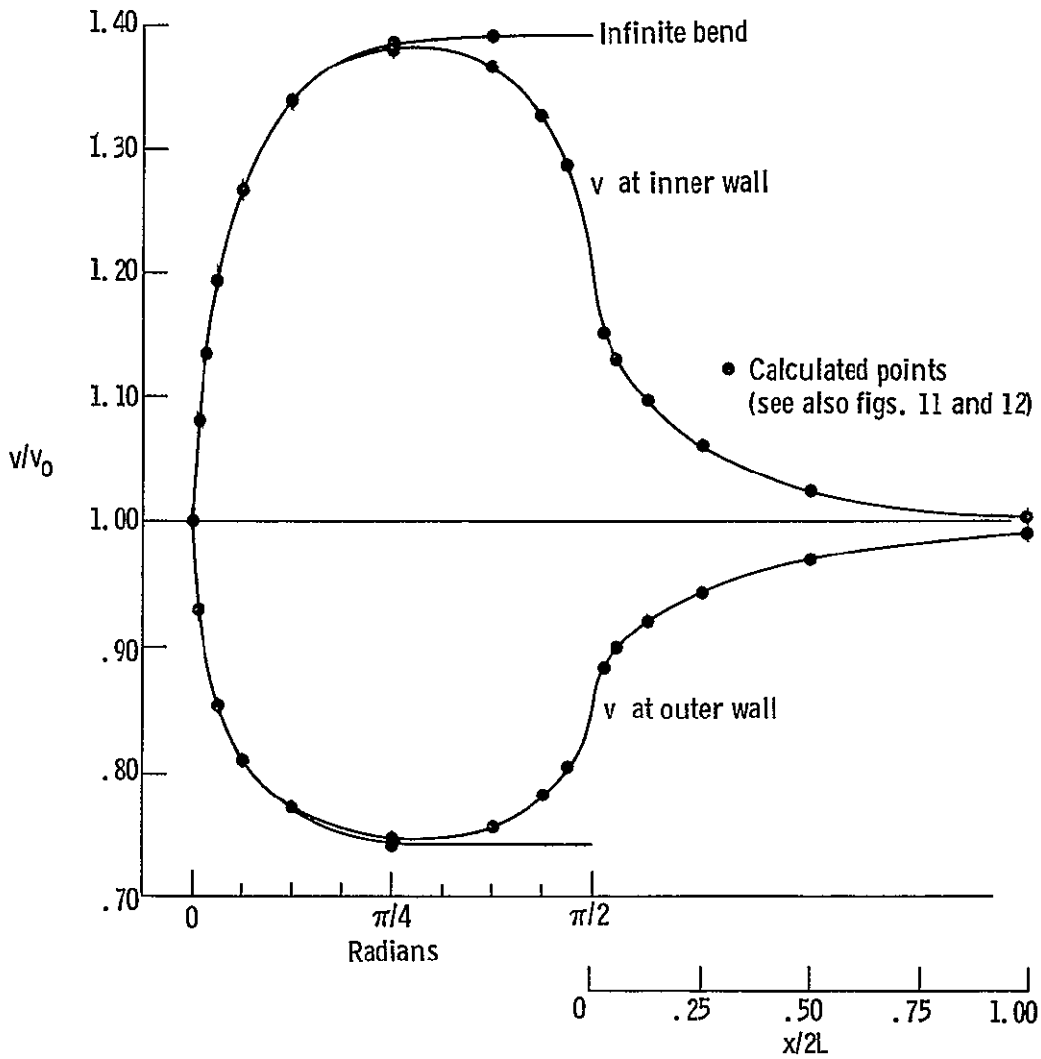


Figure 14. - Propagation in bend-straight duct system. Tangential vibrational velocities at bend's curved walls, at $r = R_1$ and $r = R_2$.

the vibrational velocities at the walls of the straight duct are, within a fraction of a percent, equal to v_0 .

For comparison purposes, the two tangential lines shown indicate the values of the vibrational velocities for an infinite bend. This graph should be compared with the well known and often published curves for potential fluid flow in elbows. Those curves give the fluid velocities of the streamlines at elbow walls, as estimated by semi-graphical solutions. The calculated curves on figure 14 are similar. The derived deviations from a logarithmic distribution of velocities in a bend are in the case of long wave motion, too small to be noticeable.

5.0 CONCLUDING REMARKS AND RECOMMENDATIONS

Propagation of long waves in a two-dimensional system has been analyzed. The acoustic approximation has been used and the Helmholtz equation was integrated for two sets of boundary conditions. The two physical systems taken into consideration are: an infinite bend approximating a coil and a 90° bend followed by a straight, infinite duct approximating a typical industrial piping system.

Implicitly the analysis gives also a solution for a system consisting of an infinite duct connected to a 90° elbow followed by a second infinite duct. The results of the analysis indicate that bending of a straight duct profoundly modifies the propagation of waves in that duct. The bend engenders the following phenomena:

- a) a set of attenuated axial and radial waves which modify the plane wave generated at the duct's inlet (figs. 5 and 6).
- b) a continuous radial, standing wave whose radial vibrations are sustained by the curvature of the bend. In a straight duct these vibrations would be quickly attenuated (fig. 7).
- c) a vortex-type distribution of the tangential vibrational velocities (fig. 3).

- d) an increase in the phase velocity which is proportional to the sharpness of the bend (fig. 4).
- e) a decrease of the amplitude of the transmitted wave. The radial reflections at the bend make the transmitted wave weaker than it was before.

The analytical results have been qualitatively verified by data obtained by Lippert⁽²⁵⁾. In spite of the differences between the system considered in the analysis and the system which has been used in experiments there is an agreement on the trend of the change of parameters of the waves crossing those bends.

The presented analysis is not directly applicable to real flows because it is based on a linearized equation valid for acoustical waves in stationary medium only. It gives, however, an idealized picture of wave's behavior in bends, in general. This work establishes a method to estimate capability of bends to transmit waves. It may be useful in the design of rigid acoustical duct systems. It also opens possibility to calculate transmittability of non-rigid bends which induce large but as yet not calculable phase changes in the progressing waves.

The obtained results should also be useful in advancing the theory of waveguides in electromagnetic application. In spite of the fact that the electromagnetic theory is concerned with high frequencies only, the developed reactions, particularly for the decaying field of velocities, should be of value. In the field of low frequency oscillations, analysis of the observed "Pogo"

instabilities of rocket systems should benefit from the developed equations. While older rocket designs were provided with straight feed piping systems, the newer designs will have bends and elbows which must be analyzed.

A more complete research may now be suggested to get a better understanding of the phenomena associated with the propagation of pulsating flows in curved pipes. From the stability of flow viewpoint the most interesting case to investigate would be a free piping system, (i.e., a bend in a piping system with one or two degrees of freedom). Across the elbow an important phase change should be obtained. From the heat transfer point of view it might be interesting to solve a tri-dimensional Helmholtz equation and wave propagation combined with fluid flow.

BIBLIOGRAPHY

1. J.W.S. Rayleigh, "The Theory of Sound", vol. II, Dover Publ., New York, 1945.
2. A. Kalahne, "Electrische Schwingungen in Ringformigen Metall Rohren", Ann. Physik, vol. 18, 1905.
3. Marc Jouguet, "Sur la propagation des ondes electromagnetiques dans les tuyaux courbes", Comptes Rendus. Academie des Sciences, v. 220, 1946, pp. 440-442.

and "Sur la propagation dans des guides courbes a section circulaire", Comptes Rendus, Academie des Sciences, v. 224, 1947, pp. 549-551.
4. Gilbert Karpman, "Onde de compression dans un fluide contenu dans un tore rigide a section carree", Comptes Rendus, Academie des Sciences, 1956, pp 770-773.
5. Georg Goubau, "Electromagnetic Waveguides and Cavities", Pergamon Press, 1961.
6. M. Matchinski, "Propagation of Sound Waves in Bent Tubes", J. Appl. Phys.; v. VII, 1930, pg 1-19.
7. Herbert Buchholz, "Der Einfluss der Krümmung von rechteckigen Hohlleitern auf das Phasenmass ultrakurzer Wellen", Electriche Nachrichten-Technik, v. 16, no. 3, 1939, 73-85.
8. P.E. Krasnushkin, "On Waves in Curved Tubes", Uchenye Zapiski, MGU, no. 75, Book 2, Part 2, 1945, pp 9-27.
9. F.E. Grigor'yan, "Theory of Sound Wave Propagation in Curvilinear Waveguides", Akusticheskii Zhurnal, v. 14, no. 3, 1968, pp 376-384 (Sov. Phys. - Acoust., v. 14, no. 3, 1969, pp. 315-321).
10. I.A. Victorov and O.M. Zubova, "Normal Plate Modes in a Solid Cylindrical layer", Akusticheskii Zhurnal, v. 9, no. 1, 1963, pp 19-22 (Sov. Phys. - Acoust., v. 9, no. 1, 1963, pp 15-17).
11. G.N. Watson, "A Treatise on the Theory of Bessel Functions" Cambridge University Press, 1962.
12. D.I. Voskresenskii, "Uniformly Curved Waveguide of Rectangular Cross Section", Trudy Moskovskogo Aviatsionnogo Inst. im.S. Ordzhonikidze, v. 73, 1957, pp 5-44.

13. A.G. Sveshnikov, B.I. Volkov and S. Ya. Sekerzh-Zenkovich, "On Bending of Waveguides", Computational Center of MGU, Collected Papers, v. 5, 1966, pp 210-226.
14. S.O. Rice, "Reflections from Circular Bends in Rectangular Wave Guides - Matrix Theory", Bell System Technical J., v. 28, April 1948, pp 305-349.
15. B. Arlinger, "Three-Dimensional Compressible Potential Flow in a Curved Duct", Ingenieur-Archiv, v. XXXVII, 1969, pp 374-387.
16. James McMahon, "On the Roots of the Bessel and Certain Related Functions", Annals of Math., v. IX, 1894, pp 23-30.
17. Rohn Truell, "Concerning the Roots of $J'_n(x) N'_n(kx) - J'_n(kx) N'_n(x) = 0$ ", J. App. Phys., v. 14, 1943, pp 350-352.
18. H.B. Dwight, "Table of Roots for Natural Frequencies in Coaxial Type Cavities", J. Math. & Phys., v. XXVII, 1948, pp 84-86.
19. Morris Kline, "Some Bessel Equations and Their Application to Guide and Cavity Theory", J. Math. & Phys., v. XXVII, 1948, pp 37-48.
20. F. Buckens, "Tables of Bessel Functions of Imaginary Order", Institut de Mecanique et Mathematiques Appliquees, Univesite Catholique de Louvain, Belgium, 1963.
21. John Miles, "The Analysis of Plane Discontinuities in Cylindrical Tubes", J. Acoust. Soc. of Am., v. 17, pp 259-272 and 272-285.
22. John Miles, "The Diffraction of Sound Due to Right-Angled Joints in Rectangular Tubes, J. Acoust. Soc. of Am., vol. 19, 1947, pp 572-579.
23. W.K.R. Lippert, "A Method of Measuring Discontinuity Effects in Ducts", Acustica, v. 4, 1954, pp 307-312.
24. W.K.R. Lippert, "The Measurement of Sound Reflection and Transmission at Right-Angled Bends in Rectangular Tubes", Acustica, v. 4, 1954, pp 313-319.
25. W.K.R. Lippert, "Wave Transmission Around Bends of Different Angles in Rectangular Ducts, Acustica, v. 5, 1955, pp 274-278.
26. P. Morse and H. Feshbach, "Methods of Theoretical Physics", Parts I and II, McGraw-Hill Book Company, Inc., New York, 1953.

27. R.J. Blade, W.-Lewis and J.H. Goodykoontz, "Study of Sinusoidally Perturbated Flow in a Line Including 90° Elbow with Flexible Supports", NASA TN D-1216, 1962.
28. Sir Horace Lamb, "Hydrodynamics", Dover Publications, New York, 1945.
29. P. Morse and K. Uno Ingard, "Linear Acoustic Theory", Handbuch der Physik, Band XI/1, Springer Verlag, 1961.
30. W.G. Penny and A.T. Price, "The Diffraction Theory of Sea Waves and the Shelter Afforded by Breakwaters", Phil. Trans. R. Soc. Lon. Series A, vol. 244, 1952.
31. R.W. Wood, "Physical Optics", The Macmillan Co., 1934.
32. "Handbook of Mathematical Functions", US Dept. of Commerce, Nat. Bureau of Standards, Applied Math. Series, 55, 1964.
33. M. Bocher, "On Some Applications of Bessel's Functions With Pure Imaginary Index", Annals of Math. VI, 1892, pp. 137-110.

APPENDIX 1

The Equation of Continuity

We define dilation $\delta = (v - v_0)/v_0$ where v is an elementary volume and the subscript zero refers to the initial state. If ζ_i are displacements in three-dimensional space

$$\delta = \frac{\partial \zeta_1}{\partial x} + \frac{\partial \zeta_2}{\partial y} + \frac{\partial \zeta_3}{\partial z}$$

The coefficient of compressibility of the fluid under consideration is defined by

$$\chi = - \frac{v - v_0}{v_0 (P - P_0)}$$

hence

$$P = P_0 - \frac{\delta}{\chi} \quad \text{and} \quad \frac{\partial P}{\partial t} = - \frac{1}{\chi} \operatorname{div} \bar{V} \quad (\text{A1.1})$$

where \bar{V} is the velocity vector. Flow of material out of the elementary volume reduces the pressure of the compressible fluid. The rate of change of excess pressure is proportional to the divergence of \bar{V} . For incompressible fluid $\operatorname{div} \bar{V} = 0$.

For an isentropic process $pv^\gamma = \text{const}$ and $v dp + \gamma p dv = 0$ and considering the definition of χ

$$\chi = - \frac{dv}{v dp} = \frac{1}{\gamma p}$$

If we put $\gamma \frac{p}{\rho} = c^2$ where c is the velocity of sound, as established by Laplace in 1816, we have

$$\frac{1}{\chi} = c^2 \quad (\text{A1.2})$$

APPENDIX 2

The Orthogonality Condition

Function $F_{\nu_m} = J_{\nu_m}(kr) J'_{-\nu_m}(kR_1) - J_{-\nu_m}(kr) J'_{\nu_m}(kR_1)$ for every ν_m must satisfy the Bessel Equation. Written for two different ν , ν_1 and ν_2 the two relations are:

$$F''_{\nu_1} + \frac{1}{r} F'_{\nu_1} + \left(k^2 - \frac{\nu_1^2}{r^2} \right) F_{\nu_1} = 0$$

$$F''_{\nu_2} + \frac{1}{r} F'_{\nu_2} + \left(k^2 - \frac{\nu_2^2}{r^2} \right) F_{\nu_2} = 0$$

Multiplied by rF_{ν_2} and rF_{ν_1} respectively, integrating, and remembering that

$$F'_{\nu_m}(kR_1) = F'_{\nu_m}(kR_2) = 0, \text{ we get}$$

$$-\int_{R_1}^{R_2} r F'_{\nu_1} F'_{\nu_2} dr + k^2 \int_{R_1}^{R_2} r F_{\nu_2} F_{\nu_1} dr - \nu_1^2 \int_{R_1}^{R_2} \frac{1}{r} F_{\nu_2} F_{\nu_1} dr = 0$$

and a similar equation for the second expression.. Subtracting, we obtain

$$(\nu_2^2 - \nu_1^2) \int_{R_1}^{R_2} \frac{1}{r} F_{\nu_2} F_{\nu_1} dr = 0$$

or

$$(\nu_2 + \nu_1)(\nu_2 - \nu_1) \int_{R_1}^{R_2} \frac{1}{r} F_{\nu_2} F_{\nu_1} dr = 0$$

and assuming that $v_1^2 \neq v_2^2$ we determine the orthogonality condition

$$\int_{R_1}^{R_2} \frac{1}{r} F_{v_1} F_{v_2} dr = 0 \quad (\text{A2.1})$$

From the above analysis we also conclude that no complex roots can exist. For if were such a complex root, its conjugate \bar{v} would also be a root and then $F_{\bar{v}} = \overline{F_v}$, and the product $F_v F_{\bar{v}}$ would be necessarily a positive number, different from zero. Consequently, v_m must have either a pure imaginary value or real values for otherwise

$$v_2^2 - v_1^2 = \bar{v}^2 - v^2 = (\bar{v} + v)(\bar{v} - v) = 4\text{Re}v\text{Im}v$$

would not vanish.

It should be pointed out that a similar relation but for Bessel functions of pure imaginary argument (ikr) has been discussed by Bocher⁽³³⁾.

APPENDIX 3

The Integral $\int F_v^2/r \, dr$

Function $F_v = J_\nu(kr)J'_{-\nu}(kR_1) - J_{-\nu}(kr)J'_\nu(kR_1)$ satisfies the Bessel equation

$$F_v'' - \frac{1}{r} F_v' + \left(k^2 - \frac{\nu^2}{r^2}\right) F_v = 0 \quad (\text{A3.1})$$

Let us differentiate (A3.1) with respect to ν and put

$$F'(\nu) = \frac{\partial F_v}{\partial \nu}$$

$$F_v'' + \frac{1}{r} F_v' + k^2 F_v - \frac{\nu^2}{r^2} F_v - \frac{2\nu}{r^2} F_v = 0 \quad (\text{A3.2})$$

Multiplying (A3.1) by rF_v and (A3.2) by rF'_ν , we have

$$\begin{aligned} \int rF_v F_v'' \, dr + \int F_v' F_v \, dr + k^2 \int rF_v F_v \, dr - \nu^2 \int \frac{1}{r} F_v F_v' \, dr \\ - 2\nu \int \frac{1}{r} F_v^2 \, dr = 0 \end{aligned}$$

$$\int rF_v F_v'' \, dr + \int F_v' F_v \, dr + k^2 \int rF_v F_v \, dr - \nu^2 \int \frac{1}{r} F_v F_v' \, dr = 0$$

Subtracting and integrating by parts the integrals containing the second derivatives of F , we have

$$rF_v F_v' \Big|_{R_1}^{R_2} - rF_v' F_v \Big|_{R_1}^{R_2} - 2\nu \int \frac{1}{r} F_v^2 \, dr = 0$$

Applying the boundary condition $F'_\nu(kR_1) = F'_\nu(kR_2) = 0$ we have,

$$\int_{R_1}^{R_2} \frac{1}{r} F_v^2 dr = \frac{1}{2v} r F_v F'_v(v) \Big|_{R_1}^{R_2}$$

where

$$F'_v(v) = \frac{\partial^2 F}{\partial r \partial v} = \frac{\partial J'_v(kr)}{\partial v} J'_{-v}(kR_1)$$

$$+ J'_v(kr) \frac{\partial J'_{-v}(kR_1)}{\partial v} - \frac{\partial J'_{-v}(kr)}{\partial v} J'_v(kR_1) - J'_{-v}(kr) \frac{\partial J'_v(kR_1)}{\partial v}$$

APPENDIX 4

The Integral $\Lambda_{mn} = \int_{R_1}^{R_2} \cos \left[\zeta_n (r - R_1) \right] \cos \left[\mu_m \ln \frac{r}{R_1} \right] dr$

The symbol Λ'_{mn} stands for the integral

$$\int_{R_1}^{R_2} \cos \left[\zeta_n (r - R_1) \right] \cos \left[\mu_m \ln \frac{r}{R_1} \right] dr$$

which is part of integral

$$\Lambda_{Fmn} = \int_{R_1}^{R_1} F_{\nu_m}(r) \cos \left[\zeta_n (r - R_1) \right] dr, m \neq 0.$$

The integral Λ_{Fmn} and, ipso facto, the integral Λ_{mn} appear in equations (1.40) and (1.41). The integral Λ_{mn} has no simple solution; however, the integral Λ_{Fmn} will be easily obtained when the basic integration of Λ_{mn} will be performed.

The problem is thus reduced to evaluation of Λ_{mn} . The process of integration of the definite integral Λ_{mn} begins with trigonometric transformation to split the integrand into four definite integrals of products of sine and cose of $(\zeta_n r)$ and $\mu_m \ln r$. Next, expanding $\cos \zeta_n r$ and $\sin \zeta_n r$ in series we obtain four alternating series containing integrable terms of the types

$$\pm \frac{\zeta_n^p}{p!} \int_{R_1}^{R_2} r^p \frac{\cos \mu_m \ln r}{\cos \mu_m \ln r} dr$$

Using the definite integrals developed earlier, equation (), and applying the integration limits, after simplification, we finally obtain

$$\Lambda_{mn} = R_1 \cos(\zeta_n R_1) \left\{ \frac{1}{1 + \mu_m^2} [a \cos(m\pi) - 1] \right. \\ - \frac{\zeta_n^2}{2!} \frac{3R_1^2}{(3^2 + \mu_m^2)} [a^2 \cos(m\pi) - 1] \\ + \left. \frac{\zeta_n^4}{4!} \frac{5R_1^4}{(5^2 + \mu_m^2)} [a^5 \cos(m\pi) - 1] - \dots \right\} + \\ + R_1 \sin(\zeta_n R_1) \left\{ \frac{\zeta_n 2R_1}{(2^2 + \mu_m^2)} [a^2 \cos(m\pi) - 1] \right. \\ - \frac{\zeta_n^3}{3!} \frac{4R_1^3}{(4^2 + \mu_m^2)} [a^4 \cos(m\pi) - 1] \\ + \left. \frac{\zeta_n^5}{5!} \frac{6R_1^5}{(6^2 + \mu_m^2)} [a^6 \cos(m\pi) - 1] - \dots \right\}$$

where $m = 1, 2, 3 \dots$ $n = 1, 2, 3 \dots$

$$\mu_m = m \frac{\pi}{\ln a} \quad \zeta_n = n \frac{\pi}{R_2 - R_1} \quad a = \frac{R_2}{R_1}$$

For the numerical application $\pi/\ln a = 5$,

$$R_2 - R_1 = 0.17489m, \quad R_1 = 0.2m$$

The derived series solution for Λ_{mn} is difficult to handle. The two converging series exhibit behavior similar to that of the series of sine and cosine of argument $\gg 1$. The second and several

following terms of the series grow very fast and attain very high values before the factorials in the denominators force the decrease of the terms.

An attempt was made to compute Λ_{mn} on a digital computer, IBM 7094 Mod II. Good results were obtained for values of $m = 1, 2, 3 \dots 6$ and for $n = 1$ and 2 . For $n = 3$ the results were erratic and for $n > 3$ even the double precision was not sufficient to carry out calculation and completely erroneous results were printed out.

A second approach consisted in use of an existing routine, recorded on tape, of integration by Simpson's Rule. A complete set of values was obtained for n and m up to 6 and in order to study the behavior of the function several values for higher n and m . All calculated Λ_{mn} are reported on figure 15. The complete set of results is presented in the form of a matrix:

Values of Λ_{mn}						
	$n = 1$	$n = 2$	$n = 3$	$n = 4$	$n = 5$	$n = 6$
$m = 1$	0,08583	0.01041	0.00140	0.000509	0.000148	0.0000849
$m = 2$	-0.02263	0.08187	0.02076	0.004048	0.00144	0.000466
$m = 3$	0.00324	-0.03208	0.07523	0.02976	0.00762	0.00276
$m = 4$	-0.00232	0.00667	-0.04069	0.06633	0.03715	0.01189
$m = 5$	0.00054	-0.00319	0.01109	-0.04774	0.05559	0.04262
$m = 6$	-0.000797	0.000934	-0.00463	0.01620	-0.05285	0.04350

Along the principal diagonal Λ_{mn} steadily decrease. Along the super and sub-diagonals the values of Λ_{mn} increase, with Λ_{mn}

for $m = n$ varying along two sine curves. By $m = n = 6$ the matrix is approximately tridiagonal. Figure 15 shows a series of functions $A_n f(m)$ which are rapidly attenuated for $n < 3$ but exhibit large oscillations for higher values of n . The values calculated by Simpson's Rule agree well with values obtained by the series solution for $n = 1$ and 2.

For $n = 1$ and $m = 1 \dots 6$ we have

m	1	2	3	4	5	6
Series solution	0.08583	-0.02263	0.00324	-0.00232	0.00054	-0.000797
Simpson's Rule	0.08577	-0.02266	0.00327	-0.00234	0.00055	-0.000804

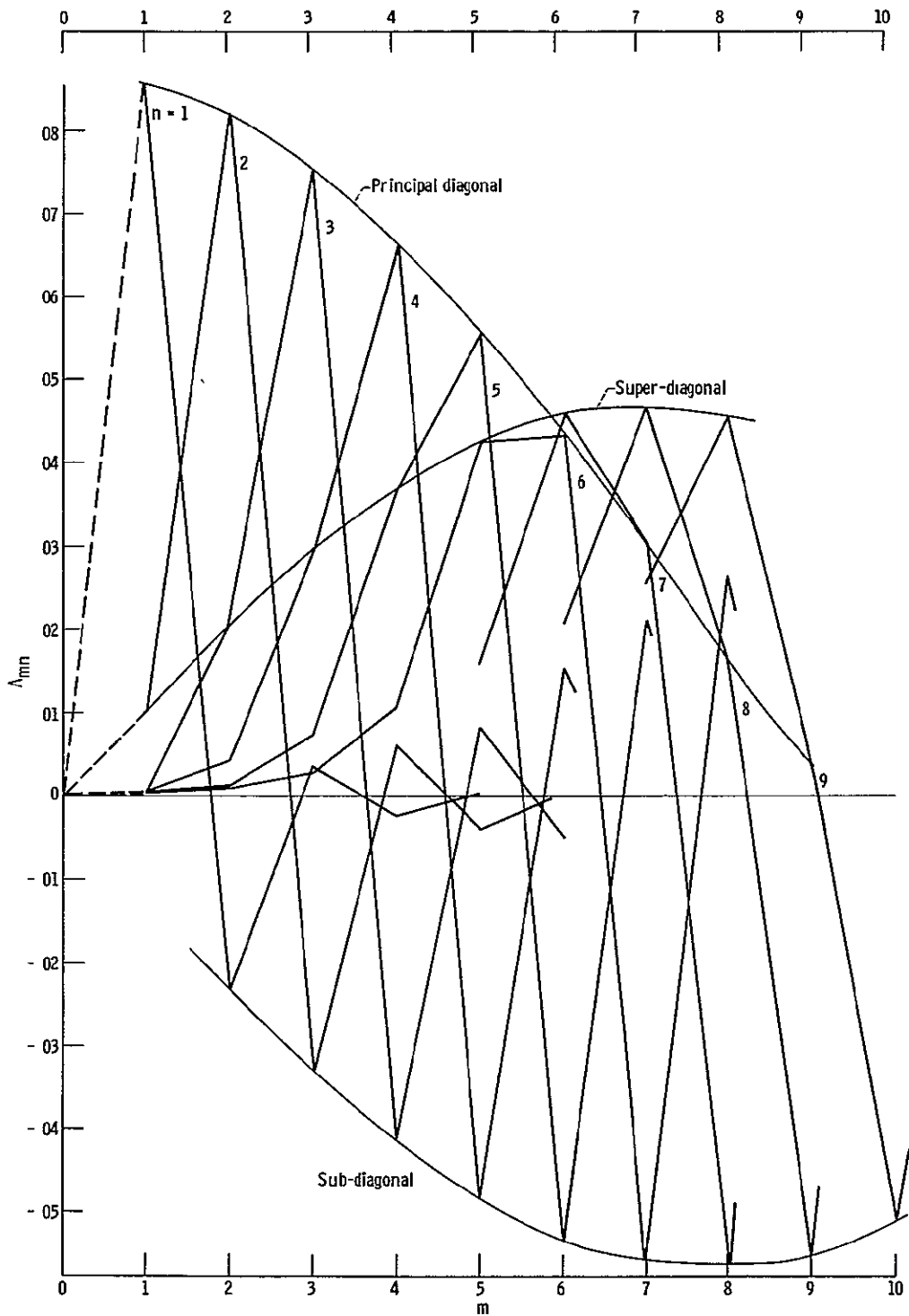


Figure 15 - Matrix of integrals $\Lambda_{mn} = \int_{R_1}^{R_2} \cos[\xi_n(r - R_1)] \cos[\mu_m \ln(r/R_1)] dr$